ALGORITHM FOR RESOLUTION IMPROVEMENT OF IMAGES

A DISSERTATION

Submitted in partial fulfillment of the requirements for the award of the degree of

MASTER OF TECHNOLOGY

in

ELECTRICAL ENGINEERING

(With Specialization in Measurement and Instrumentation)

By

VENKATA GOURI RAJESH E

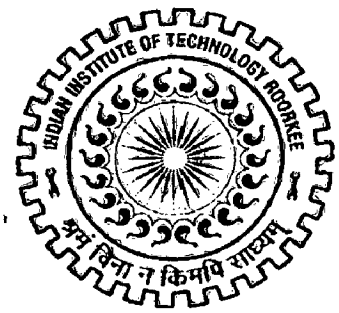

DEPARTMENT OF ELECTRICAL ENGINEERING
INDIAN INSTITUTE OF TECHNOLOGY ROORKEE
ROORKEE - 247 667 (INDIA)

JUNE, 2007

INDIAN INSTITUTE OF TECHNOLOGY ROORKEE
ROORKEE

CANDIDATE'S DECLARATION

I hereby declare that the work, which is being presented in this dissertation entitled **ALGORITHM FOR RESOLUTION IMPROVEMENT OF IMAGES** in the partial fulfillment of the requirements for the award of the degree of **Master of Technology in Electrical Engineering** with specialization in **Measurement and Instrumentation,** in the **Department of Electrical Engineering,** Indian Institute of Technology Roorkee, Roorkee is an authentic record of my own work carried out during a period from July 2006 to June 2007 under the supervision of **Dr. Vinod Kumar,** Professor, Electrical Engineering Department, Indian Institute of Technology Roorkee, Roorkee and **Dr.Ila Gupta,** Assistant Professor, Department of Architecture & Planning, Indian Institute of Technology Roorkee, Roorkee .

The matter presented in this thesis has not been submitted by me for the award of any other degree of this or any other Institute.

E.V.G. Rajesh

Date: 25-06-07 **(VENKATA GOURI RAJESH E)**

Place: Roorkee

CERTIFICATE

This is to certify that the above statement made by the candidate is correct to the best of my knowledge and belief.

Ila Gupta. 25.6.07

Dr.Ila Gupta,
Assistant Professor,
Department of Architecture & Planning,
Indian Institute of Technology,
Roorkee-247667, India.,

25/6/07

Dr. Vinod Kumar
Professor,
Department of Electrical engineering,
Indian Institute of Technology
Roorkee-247667, India.

ACKNOWLEDGEMENTS

I express my foremost and deepest gratitude to **Dr. Vinod Kumar**, Professor, Department of Electrical Engineering, Indian Institute of Technology Roorkee, Roorkee and **Dr.Ila Gupta**, Assistant Professor, Department of Architecture & Planning, Indian Institute of Technology Roorkee, Roorkee, for his valuable guidance, support and motivation throughout this work. I have deep sense of admiration for his innate goodness and inexhaustible enthusiasm. The valuable hours of discussion and suggestions that I had with him have undoubtedly helped in supplementing my thoughts in the right direction for attaining the desired objective. I consider myself extremely fortunate for having got the opportunity to learn and work under his able supervision over the entire period of my association with him.

My sincere thanks to all faculty members of Measurement & Instrumentation for their constant encouragement, caring words, constructive criticism and suggestions towards the successful completion of this work.

I do acknowledge with immense gratitude the timely help and support, which I received from my classmates and the Research Scholars in the "Instrumentation and Signal Processing Laboratory". I am also thankful to the staff of this Lab for their kind cooperation.

Last but not least, I'm highly indebted to my parents and family members, whose sincere prayers, best wishes, moral support and encouragement have a constant source of assurance, guidance, strength, and inspiration to me.

(Venkata Gouri Rajesh E)

ABSTRACT

The process of constructing high resolution image from low resolution images is called ***superresolution.*** To achieve these algorithms precise registration algorithms to align low resolution images are needed.

The low resolution images are Undersampled which have the problem of aliasing and misregistered. So as to overcome the problem of aliasing it uses the low frequency aliasing free part of the image is used for registration algorithm. The registration algorithms that are used are broadly divided in to spatial and frequency domain. Here new type of frequency domain method is used. This registration method uses a one dimensional correlation where as other methods uses two dimensional correlation. So obviously the execution time of the algorithm will be lesser compared to other methods. A high-resolution image is then reconstructed using cubic interpolation.

After implementing the output image of this method is compared with the original high resolution image, and also with the conventional interpolation techniques and errors are compared.

CONTENTS

List of Figures

List of Tables

CHAPTER 1

INTRODUCTION

1.1 Overview

The term *image resolution* is defined as the smallest discernible or measurable detail in a visual presentation. Resolution refers to the spacing of pixels in an image and is measured in pixels per inch (ppi). The higher the spatial resolution, the greater the number of pixels in the image and correspondingly, the smaller the size of individual pixels will be. This allows for more detail and subtle color transitions in an image. The spatial resolution of a display device is often expressed in terms of dots per inch (dpi) and it refers to the size of the individual spots created by the device. The intermediate pixel values can be found by a single low resolution frame using interpolation techniques. In this process the resolution is appeared to be improved. Because there is no new information supplied with the single image and also we can not create new information. So as to get the true resolution enhancement a number of misregistered and aliased low resolution frames are to be taken. The term misregistration and aliasing will be explained later. The process of constructing a high resolution image form the set of low resolution frames is called ***superresolution.***

1.2 Motivation of Work

Sensor with a high density of photo-detectors captures images at a high spatial resolution. But a sensor with few photo-detectors produces a low resolution image leading to pixelization where individual pixels can be seen with the naked eye. This follows from the sampling theorem according to which the spatial resolution is limited by the spatial sampling rate, i.e., the number of photo-detectors per unit length along a particular direction. Another factor that limits the resolution is the photo-detector's size. One could think of reducing the area of each photo-detector in order to increase the

number of pixels. But as the pixel size decreases, the image quality is degraded due to the enhancement of shot noise. It has been estimated that the minimum size of a photo detector should be approximately $50\mu m^2$.

There is a broad usage of super resolution. This is mainly used in military application and LANDSAT applications. In military surveillance a low resolution camera is sent along with surveillance air craft to capture multiple pictures. This is done because the battery life is major problem in LANDSAT and military applications as high resolution cameras consume more energy than low resolution cameras. This can also be used in License plate readers, surveillance monitors, and medical imaging applications.

1.3 **Objective**

Given a set of four aliased misregistered low resolution (LR frames) input images called frames and also resolution enhancement factor, the goal is to construct a high resolution image (HR frame) also called high resolution frame form the set of these LR fames. The input images that are supplied are misregistered and aliased.

Along with low resolution images an original high resolution image of the same scene is also taken with a high resolution camera. After achieving the super resolution image from the set of low resolution images, error between the resolution enhanced image and original image is to be calculated. The error of the implemented algorithm is compared with the errors of the images obtained from the conventional interpolation algorithms which use a single low resolution image as input.

1.4 **Literature Survey**

The idea of super-resolution was first introduced in 1984 by Tsai and Huang [8] for multiframe image restoration of bandlimited signals. A good overview of existing algorithms is given by Borman and Stevenson [11] and Park et al. [12]. Most super-resolution methods are composed of two main steps: first all the images are aligned in the same coordinate system in the registration step, and then a high-resolution image is

reconstructed from the irregular set of samples. In this second step, the camera point spread function is often taken into account. Precise subpixel image registration is a basic requirement for a good reconstruction. If the images are inaccurately registered, the high-resolution image is reconstructed from incorrect data and is not a good representation of the original signal.

Tsai and Huang [8] describe an algorithm to register multiple frames simultaneously using nonlinear minimization in frequency domain. Their method for registering multiple aliased images is based on the fact that the original, high resolution signal is bandlimited. It is not clear, however, if such a solution is unique and if such an algorithm will not converge to a local minimum. Most of the frequency domain registration methods are based on the fact that two shifted images differ in frequency domain by a phase shift only, which can be found from their correlation. Using a log polar transform of the magnitude of the frequency spectra, image rotation and scale can be converted into horizontal and vertical shifts. These can therefore also be estimated using a phase correlation method.

Reddy and Chatterji [13] describe such planar motion estimation algorithms. Reddy and Chatterji apply a high-pass emphasis filter to strengthen high frequencies in the estimation. To minimize errors due to aliasing, their methods rely on a part of the frequency spectrum that is almost free of aliasing. Typically this is the low-frequency part of the images. Foroosh et al. [14] showed that the signal power in the phase correlation corresponds to a polyphase transform of a filtered unit impulse. Lucchese and Cortelazzo [15] developed a rotation estimation algorithm based on the property that the magnitude of the Fourier transform of an image and the mirrored version of the magnitude of the Fourier transform of a rotated image has a pair of orthogonal zero-crossing lines. The angle that these lines make with the axes is equal to half the rotation angle between the two images. The horizontal and vertical shifts are estimated afterwards using a standard phase correlation method. Spatial domain methods generally allow for more general motion models, such as hymnographies.

The implemented technique uses new frequency domain algorithm [6] to register not just low resolution, but also aliased images. Planar motions are allowed. When a series of images is taken in a short amount of time with only small camera motion between the images, we assume that the motion can be described with such a model. In general, a planar model is simpler and has less parameter making it often more robust in the presence of noise.

1.4 **Organization of Thesis**

The entire thesis is organized in 5 chapters:

Chapter two gives idea of basic conventional interpolation techniques, their advantages and disadvantages.

Chapter three gives idea of generalized super resolution schema with the help of block diagram. This chapter also gives significance of each block registration, restoration and post processing.

Chapter four gives full idea of the implemented frequency domain approach.

Chapter five covers the results and discussion of the implemented method to the conventional methods. It also covers the performance improvement.

CHAPTER 2
INTERPOLATION TECHNIQUES

2.1 Introduction

Interpolation means Guessing at the function values within the known range. Interpolation has great significance in general image/video processing. If input image of size N*N, so as to construct an image of size kN*kN intensity values at intermediate pixel locations has to be estimated, this process is called interpolation. The one dimensional interpolation scheme is shown in the diagram fig 2.1.

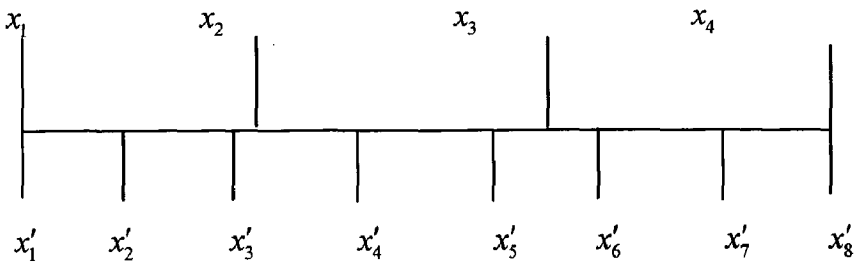

Figure 2.1 One Dimensional Interpolation

Where X are original points

X' Are interpolated points

The basic two dimensional interpolations are shown in the fig 2.2 where input image is of size 4*4 and interpolated image is of 8*8 sizes.

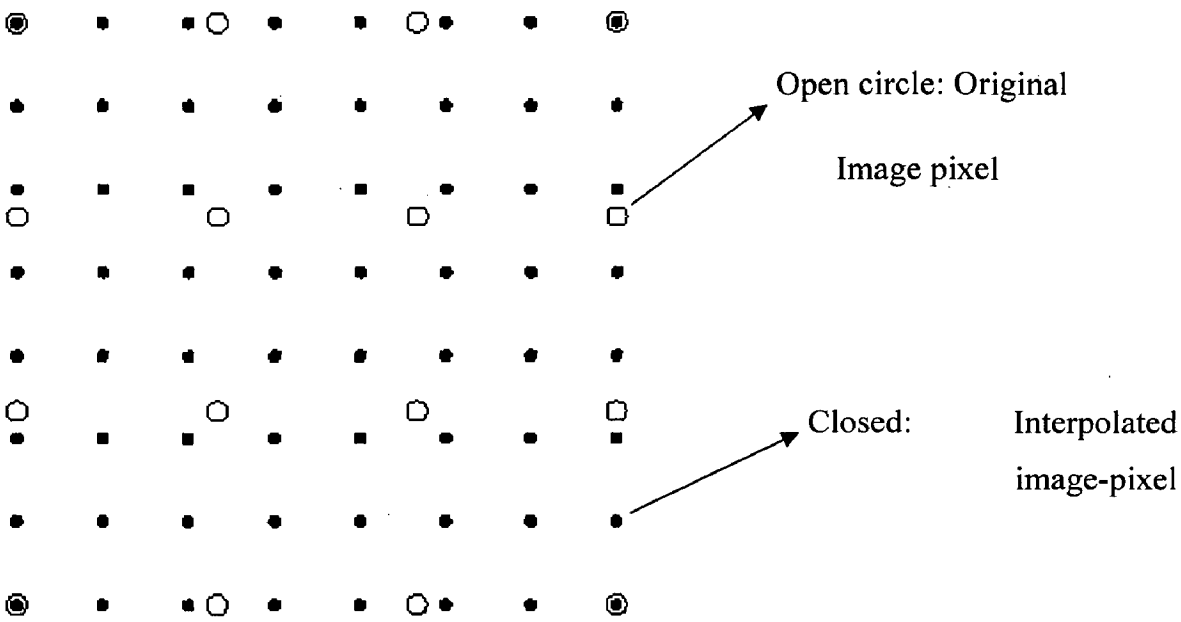

Figure 2.2 Basic Image Interpolation

Types of interpolation techniques

Depending on mathematics involved in finding the pixel intensity at a particular pixel the interpolation techniques are divided in to different types. And some of the interpolation techniques are

- Nearest neighborhood interpolation
- Bilinear interpolation
- Bicubic interpolation

2.2 Nearest Neighborhood Interpolation

Nearest neighbor hood interpolation are the most basic technique and takes least processing time of all the interpolation algorithms because it only considers one pixel-- the closest one to the interpolated point. This has the effect of simply making each pixel bigger. A nearest neighbor interpolation is preferred if subtle variations in the grey

levels need to be retained, if classification will follow the registration, or if a classified image is to be re-sampled.

The nearest neighborhood interpolation for one dimension is shown below in fig 2.3.

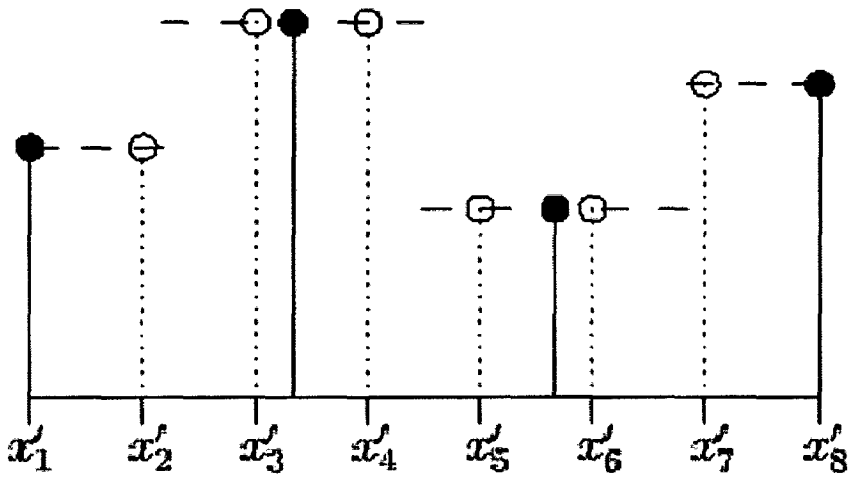

Fig 2.3 One Dimensional Nearest Neighborhood interpolation

(Solid lines –original values, Dotted lines-interpolated values)

Nearest neighbor interpolation introduces a small error into the newly registered image. The image may be offset spatially by up to 1/2 a pixel, causing a jagged or blocky appearance if there is much rotation or scale change.

2.3 Bilinear interpolation

The general idea of linear interpolation in one dimension is shown in figure 2.4. So as to calculate the intensity value F between pixels x_1 and x_2 whose intensity values are given by $f(x_1)$ and $f(x_2)$ the equation 2.1 is used.

$$\frac{F - f(x_1)}{\lambda} = \frac{f(x_2) - f(x_1)}{1} \qquad (2.1)$$

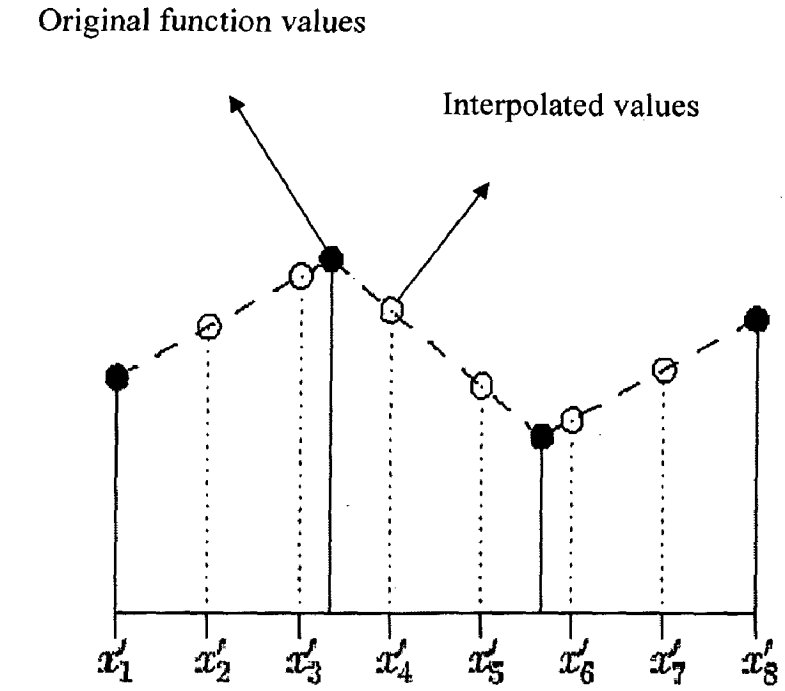

Where Solid lines original function values, Dotted lines interpolated values

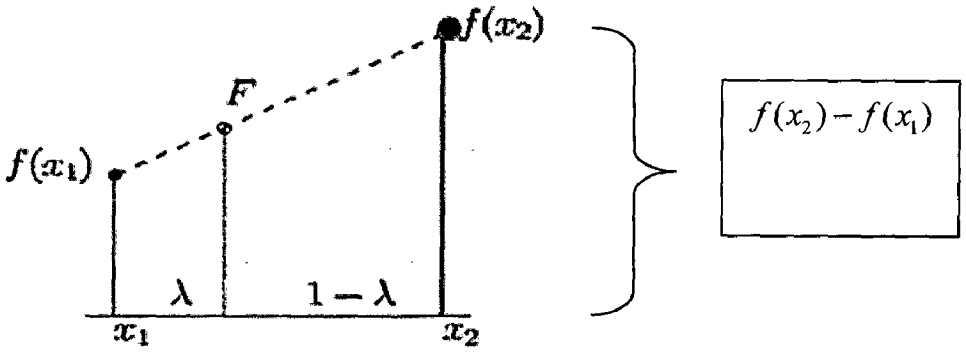

Fig 2.4 Generalized linear Interpolation in One Dimension

Bilinear interpolation considers the closest 2x2 neighborhood of known pixel values surrounding the unknown pixel. It then takes a weighted average of these 4 pixels to arrive at its final interpolated value. The idea of bilinear interpolation for an image is shown in the figure 2.5. This figure shows how an 8x8 image is constructed from a 4x4 image

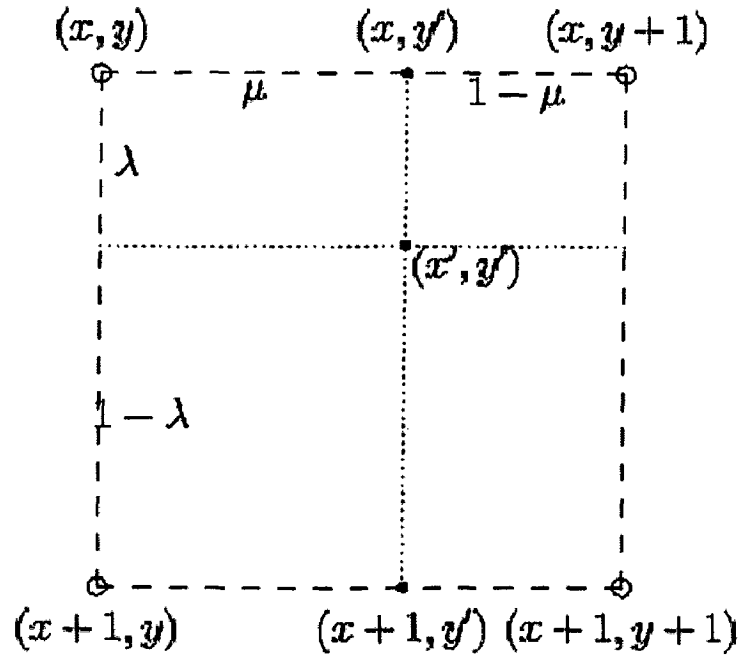

Fig 2.5 Bilinear interpolations of 8x8 images from 4x4

Where in the above figure $(x,y),(x,y+1),(x+1,y) and (x+1,y+1)$ are the four original pixel values. First the intensity value at location (x,y') is calculated from the intensity values at locations $(x,y) and (x,y+1)$. Again same process repeated to calculate intensity value at location $(x+1,y')$ from the intensity values at pixel locations $(x+1,y) and (x,y+1)$. From the calculated values of intensity at locations $(x,y') and (x+1,y')$ we will calculate the pixel intensity value of the pixel (x',y').

This above process is given by the equations 2.2

$$f(x,y') = \mu f(x,y+1) + (1-\mu) f(x,y)$$

$$f(x+1,y') = \mu f(x+1,y+1) + (1-\mu) f(x+1,y) \qquad (2.2)$$

$$f(x',y') = \lambda f(x+1,y') + (1-\lambda) f(x,y')$$

All the above equations are mixed to directly give the formulation 2.3

$$f(x',y') = \lambda\left(\mu f(x+1,y+1)+(1-\mu) f(x+1,y)\right) \qquad (2.3)$$

$$+(1-\lambda)\left(\mu f(x,y+1)+(1-\mu) f(x,y)\right)$$

Bilinear interpolation results in much smoother looking images than nearest neighbor. But the grey level values are altered in the process, resulting in blurring or loss of image resolution.

2.4 **Bicubic Interpolation**

Bicubic interpolation is the most widely used and considered as the precise interpolation suited for wide range of images. Bicubic goes one step beyond bilinear by considering the closest 4x4 neighborhood of known pixels for a total of 16 pixels.

The generalized one dimensional interpolation which uses a function R to interpolation is given by the formulation. This is shown in the figure 2.6.

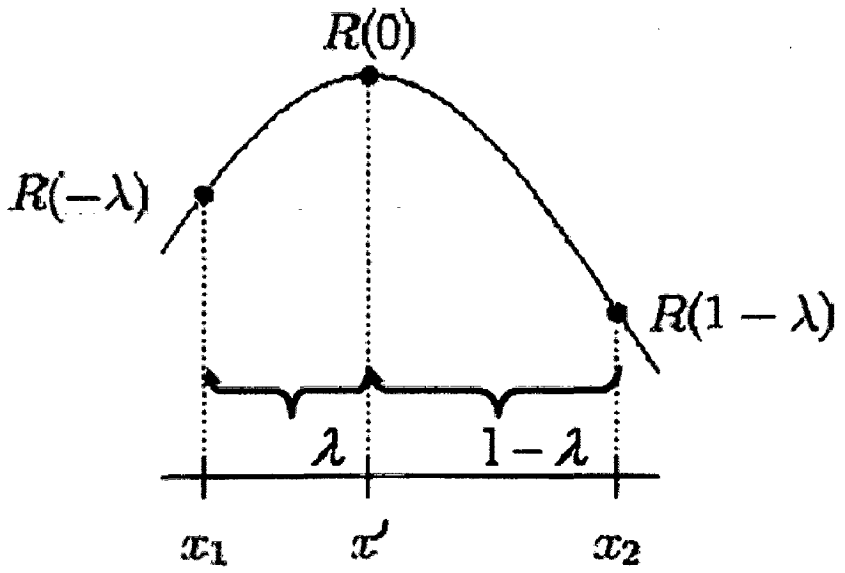

Fig 2.6 Generalized Interpolation

Depending on function R(u) the type of interpolation is determined. The function R(u) is centered at x'. Suppose if we have to interpolate a value $f(x')$ for which $x_1 < x' < x_2$ and $x' - x_1 = \lambda$. Then the interpolated value at pixel x' is given by equation 2.4.

$$f(x') = R(-\lambda) f(x_1) + R(1-\lambda) f(x_2)$$

(2.4)

This method is closer to the perfect sin(x)/x re-sampler than nearest neighbor or bilinear interpolation. Since these are at various distances from the unknown pixel, closer pixels are given a higher weighting in the calculation. It does not have the disjointed appearance produced by nearest neighbor interpolation.

Bicubic produces noticeably sharper images than the previous two methods, and is perhaps the ideal combination of processing time and output quality. For this reason it is a standard in many image editing programs. Because the grey level values are altered by this method, any image classification processes should be performed before the interpolation. Cubic convolution requires about 10 times the computation time required by the nearest neighbor method.

Bicubic interpolation fits a series of cubic polynomials to the brightness values contained in the 4 x 4 array of pixels surrounding the calculated address.

- Step 1: Four cubic polynomials $F(i), i = 0,1,2,3$ are fit to the control points along the rows. The fractional part of the calculated pixel's address in the x-direction is used. Shown in fig 2.7

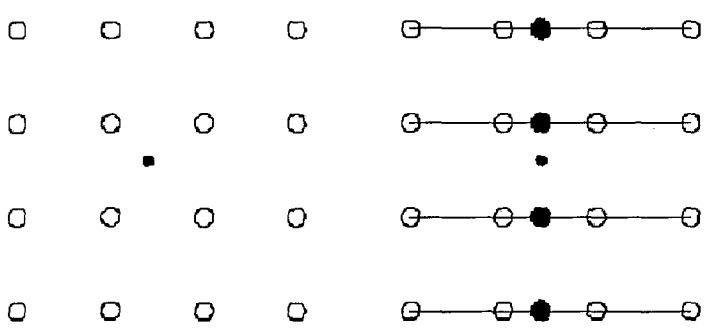

Figure 2.7 Interpolation along x-axis

- Step 2: the fractional part of the calculated pixel's address in the y-direction is used to fit another cubic polynomial down the column, based on the interpolated brightness values that lie on the curves $F(i), i = 0,1,2,3$.

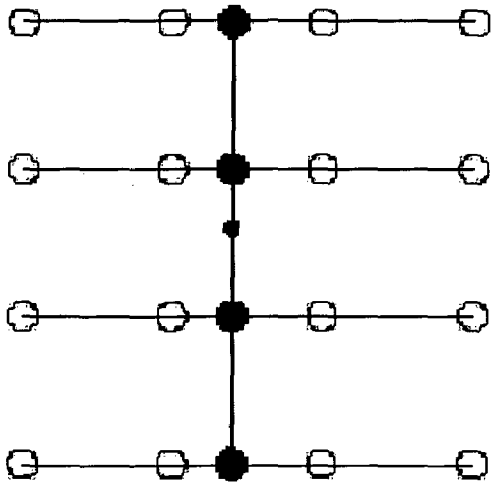

Fig 2.8 interpolation along y direction

2.5 Conclusion

This chapter gives the understanding of different types of interpolation techniques related to image processing. It gives idea about he advantages and disadvantages of each technique and also it gives idea about which interpolation technique is suitable for particular applications. This chapter gives the understanding that the number of pixels used from he neighborhood to estimate value at unknown pixel is related to the computational time of the technique.

CHAPTER 3

GENERALIZED SCHEME OF RESOLUTION ENHANCEMENT

3.1 Introduction

Previous chapter's gives understanding that we have to construct a high resolution images from the set of low resolution images. This chapter gives the explanation about the generalized resolution enhancement process and also explains the different types of technique that can be used to at each step in the basic scheme.

A set of aliased misregistered low resolution (LR frames) input images called frames are given and also resolution enhancement factor, the goal is to construct a high resolution image (HR frame) called high resolution frame form the set of these LR fames whose resolution enhancement factor is given.

3.2 Input Images

Several subsampled misregistered low resolution images of desired scene are obtained using low resolution camera. These low-resolution images can be obtained as a sequence taken over time with arbitrary translations and rotations of camera. The translational over X and Y directions are shown expressed as δ_x , δ_y . The rotation angle of the camera is expressed by the parameter θ which we don't know.

A single high-resolution frame can be constructed from low-resolution images is because the images are subsampled (aliased) as well as misregistered with sub-pixel shifts. If the images are shifted by integer amounts of pixels, then all images contains the same information (intensity values at the same spatial location), so if we go through the super resolution process there will be no improvement compared to interpolation techniques.

In addition, there is loss of high-frequency detail in LR images due to the low resolution camera and the optical blurring due to motion or out-of-focus.

The model relating a high resolution image to the low resolution observed frames is shown in Figure 3.1 as in [2]. The input signal $f(x,y)$ denotes the continuous (high

resolution) image in the focal plane co-ordinate system (x, y). Motion is modeled as a pure rotation θ_k and a translation δ_k. The shifts are defined in terms of low-resolution pixel spacing.

This step requires interpolation since the sampling grid changes in the geometric transformation. Next the effects of the physical dimensions of the low resolution sensor (i.e., blur due to integration over the surface area) and the optical blur (i.e., out-of-focus blur) are modeled as the convolution of $g_k(x, y)$ with the blurring kernel $h(x, y)$. Finally, the transformed image undergoes low-resolution scanning followed by addition of noise yielding the low resolution k^{th} frame/observation $y_k(x, y)$.

Suppose if we are taking the images by our own camera there is no need to use a tripod and give precise translations and rotations to the camera. The amount of translations that occur due to the hand movement is enough to produce desirable translations motion. It is better to construct HR frame from a large set of LR frames. The number of LR frames used will directly related to the quality of the HR frame.

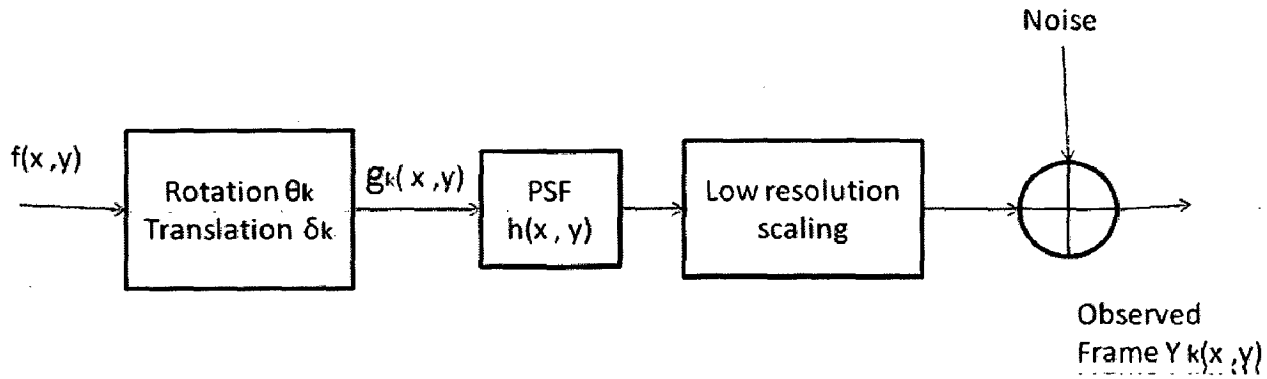

Fig 3.1 Observation model relating high resolution image to the low resolution observed frames

3.3 Generalized Block Diagram for Super Resolution

Generalize super resolution scheme from set of low resolution images can be shown by a block diagram is shown in the figure 3.2 as in [9]. They are based on the

assumption that all pixels from available frames can be mapped back onto the reference frame, based on the motion vector information, to obtain an up sampled frame, as in[8].

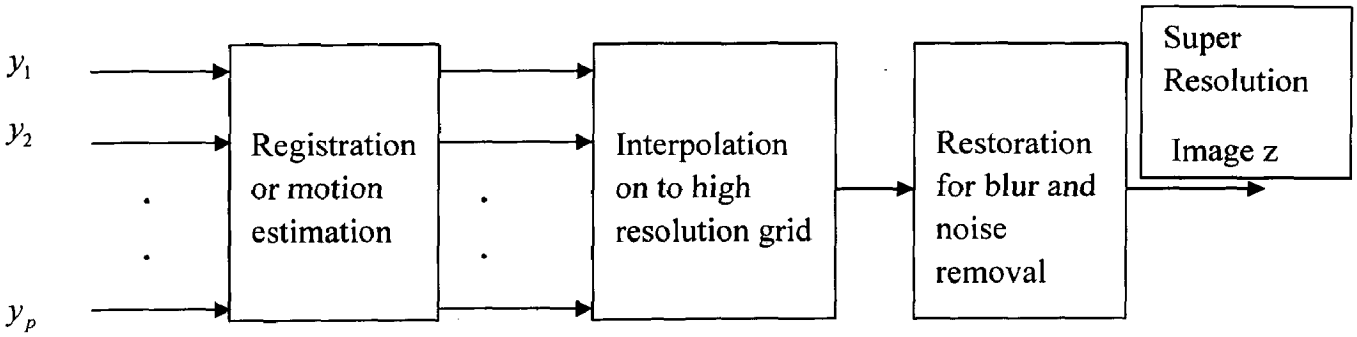

Fig 3.2 Scheme of Super Resolution from Multi-Frame Shifted Observations

3.4 Registration or Motion Estimation

This is the first and most important step in multi-frame resolution improvement. Registration is a fundamental task in image processing used to match two or more pictures taken, for example, at different times, from different sensors, or from different viewpoints. To register images, a spatial transformation is found which will remove these variations. A frequent problem arises when images taken, at different times, by different sensors or from different viewpoints need to be compared.

Depending on the type of misregistration the registration can be broadly classified to many types. They are ([4])

MULTIMODAL REGISTRATION:-

- Registration of images of the same scene acquired from different sensors.
- Application: Integration of information for improved segmentation and pixel classification.
- Field: Medical Image Analysis, Remotely Sensed Data Processing.

TEMPLATE REGISTRATION

- Find a match for a reference pattern in an image.
- Application: Recognizing or locating a pattern such as an atlas, map, or object model in an image.
- Field: Remotely Sensed Data Processing, Pattern Recognition.

VIEWPOINT REGISTRATION

- Registration of images taken from different viewpoints.
- Application: Depth or shape reconstruction.
- Field: Computer Vision, Stereo mapping to recover depth or shape from disparities. Tracking object motion; image sequence analysis may have several images which differ only slightly, so assumptions about smooth changes are justified.
- In the implemented algorithm I have considered this form of registration.

TEMPORAL REGISTRATION

- Problems: Registration of images of same scene taken at different times or under different conditions.
- Applications: Detection and monitoring of changes or growths. Field: Medical Image Analysis, Remotely Sensed Data Processing.

3.4.1 Image Transformations

As previously explained also in [4] so as to register two images first image is named as reference image and the image to be registered is called as template image. The images can be related by mathematical mapping function

$$I_2(x,y) = I_1(f(x,y)) \tag{3.1}$$

Where

$I_1(x,y)$ ---------- Reference Image

$I_2(x,y)$ ----------Template Image

f ----------Transformation function

x, y ----------Pixel Co-ordinates

In Figure 3.3, an example of several of the major transformation classes are shown. Registration, in this case, involves a search for the direction and amount of translation needed to match the images.

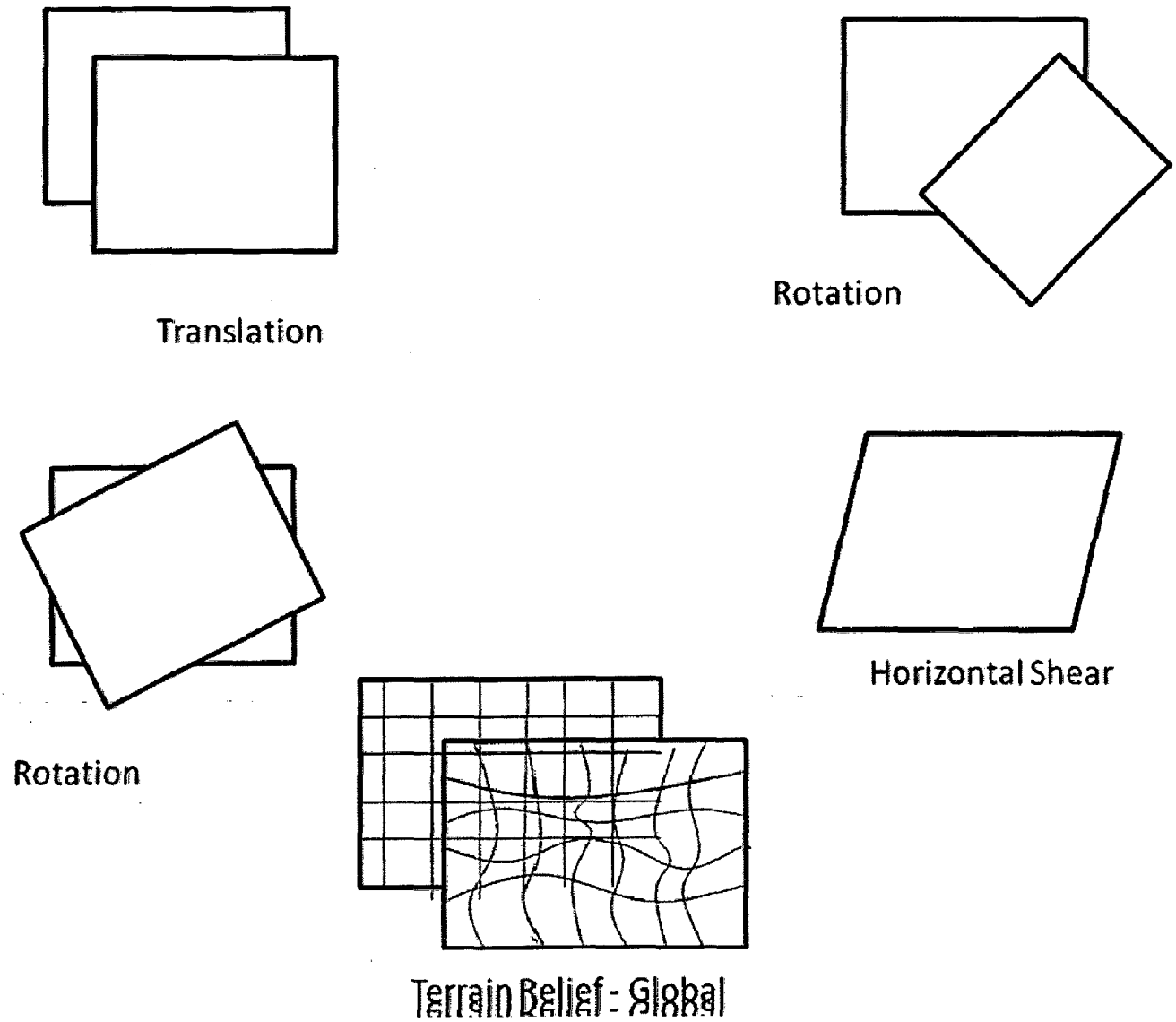

Figure 3.3 Examples of typical geometric transformations.

The transformations shown in Figure 3 are a rotational, rigid body, shear, and a more general global transformation due to terrain relief. In general, the type of transformation used to register images is one of the best ways to categorize the methodology and assist in selecting techniques for particular applications. The transformations can be global or local. Global transformations are transformations which are global to whole images where as local transformations are for a part of image. Generally there will be global transformations. A global transformation is given by a single equation which maps the entire image. Examples are the affine, projective, perspective, and polynomial transformations. Local transformations map the image differently depending on the spatial location and are thus much more difficult to express succinctly. The variations in the image here we consider are due to the changes in camera position and viewpoint.

If we define these images as two 2D arrays of a given size denoted by I_1 and I_2 where $I_1(x,y)$ and $I_2(x,y)$ each map to their respective intensity (or other measurement) values, then the mapping between images can be expressed as:

$$I_2(x,y) = g(I_1(f(x,y))) \tag{3.2}$$

Where f is a 2D spatial-coordinate transformation, i.e., f is a transformation which maps two spatial coordinates, x and y, to new spatial coordinates x' and y'.

$$(x',y') = f(x,y) \tag{3.3}$$

The registration problem is to find the optimal spatial and intensity transformations so that the images are matched either for the purposes of determining the parameters of the matching transformation or to expose differences of interest between the images. The intensity transformation is not always necessary, and often a simple lookup table determined by sensor calibration techniques & sufficient. Our aim is to find the transformation function f. Finding the parameters of the optimal spatial or transformation is generally the key to any registration problem. It is frequently expressed parametrically as two single-valued functions f_x, f_y, which may be more easily implemented.

$$I_2(x,y) = I_1(f_x(x,y), f_y(x,y))$$

(3.4)

The most common general transformations are rigid, affine, projective, perspective, and global polynomial.

- Rigid body transformations account for object or sensor movement in which objects in the images retain their relative shape and size. A rigid-body transformation is composed of combination of a rotation, a translation, and a scale change. An example is shown in fig 3.3.
- Affine transformations are more general than rigid and can therefore tolerate more complicated distortions while still maintaining some nice mathematical properties. A shear transformation, also shown in Figure 3.3, is an example of one type of affine transformation.
- Projective transformations are more general transformations of distortions due to the projection of objects at varying distances to sensor on to the image plane.

A transformation T is linear if,

$$T(x_1 + x_2) = T(x_1) + T(x_2) \tag{3.5}$$

And for every constant

$$cT(x) = T(cx)$$

A transformation is affine if $T(x) - T(0)$ is linear. Affine transformations are linear in the sense that they map straight lines into straight lines. The most commonly used registration transformation is the affine transformation which is sufficient to match two images of a scene taken from the same viewing angle but from a different position, i.e., the camera -can be moved, and it can be rotated around &s optical axis. This affine transformation is composed of the Cartesian operations of a scaling, a translation, and a rotation. It is a global transformation which is rigid since the overall geometric relationships between points do not change, i.e., a triangle in one image maps into a similar triangle in the second image.

It has four parameters t_x, t_y, s, θ, which maps a point of the first image in to a point of the second image as follows:

$$\begin{pmatrix} x_2 \\ y_2 \end{pmatrix} = \begin{pmatrix} t_x \\ t_y \end{pmatrix} + s \begin{pmatrix} \cos\theta & -\sin\theta \\ \sin\theta & \cos\theta \end{pmatrix} \begin{pmatrix} x_1 \\ y_1 \end{pmatrix} \tag{3.6}$$

This can be rewritten as

$$\bar{p}_2 = \bar{t} + sR\bar{p}_1$$

Where $\bar{p}_1, \bar{p}_2$, are the coordinate vectors of the two images,

$\bar{t}$ is the translation vector,

s is a scalar scale factor, and R is the rotation matrix.

Since the rotation matrix R is orthogonal (the rows or columns are perpendicular to each other), the angles and lengths in the original image are preserved after the registration. Because of the scalar scale factor s, the rigid-body transformation allows changes in length relative to the original image, but it is the same in both x and y. Without the addition of the translation vector, the transformation becomes linear.

3.4.2 Registration Methods

3.4.2.1 *Correlation and Sequential Methods*

Cross-correlation is the basic statistical approach to registration. If is often used for template matching or pattern recognition in which the location and orientation of a template or pattern is found in a picture. By itself, cross-correlation is not a registration method. It is a similarity measure or match metric, i.e., it gives a measure of the degree of similarity between an image and a template. It is used in several registration methods. These methods are generally useful for images which are misaligned by small rigid and affine transformations. For a template T *and* image I the two dimensional cross correlation function measures the similarity for each translation.

$$C(u,v) = \frac{\Sigma_x \Sigma_y T(x,y) I(x-u, y-v)}{\sqrt{[\Sigma_x \Sigma_y I^2(x-u, y-v)]}} \tag{3.7}$$

If the template matches the image exactly, except for an intensity scale factor, at a

translation of (i, j), the cross correlation will have peak at $c(i, j)$. Thus computing C over all possible translations, it is possible to find the degree of similarity for any template-sized window in the image. Cross correlation must be normalized since local image intensity otherwise influence the measure. In general we take measure of sum of the differences squared between the template and the picture at each location of the template. When the template is placed over the picture at location (u, v) for which the template is most similar, the differences between the corresponding intensities will be smallest.

$$D(u,v) = \sum_x \sum_y (T(x,y) - I(x-u, y-v))^2 \tag{3.8}$$

The cross-correlation between the image and the template (or one of the related similarity measures given above) is computed for each allowable transformation of the template. The transformation whose cross-correlation is the largest specifies how the template can be optimally registered to the image.

This is the standard approach when the allowable transformations include a small range of translations, rotations, and scale changes. The template is translated, rotated, and scaled for each possible translation, rotation, and scale of interest.

As the number of transformations grows, however, the computational complexity becomes high. If the image is noisy, i.e., there are significant distortions which cannot be removed by the transformation, the peak of the correlation may not be clearly distinguishable. The disadvantages of these techniques are that they can be computationally intensive, does not work properly if images have noise. The correlation methods can be used sometimes for more general rigid transformations but become inefficient as the degrees of freedom of the transformation increases.

3.4.2.2 Fourier Methods

The methods to be described in this section register images by exploiting several nice properties of the Fourier Transform. Translation, rotation, reflection, distributivity, and scale all have their counterpart in the Fourier domain. These methods differ from the correlation methods because they search for the optimal match according to information

in the frequency domain. The correlation methods described above uses Fourier transform as a tool to perform a spatial correlation. The Fourier transformation techniques are suited for frequency dependent noise effected noise.

The Fourier transform of an image is given bye the equation

$$F(\omega_x, \omega_y) = R(\omega_x, \omega_y) + iI(\omega_x, \omega_y) \tag{3.9}$$

Or alternatively it can be expressed as

$$F(\omega_x, \omega_y) = \left|F(\omega_x, \omega_y)\right| e^{j\Phi(\omega_x, \omega_y)} \tag{3.10}$$

If two images f_1 and f_2 are differed by translation displacement (d_x, d_y) which are related by formulation

$$f_2(x, y) = f_1(x - d_x, y - d_y) \tag{3.11}$$

Then the Fourier transforms are related by

$$F_2(\omega_x, \omega_y) = e^{-j(\omega_x d_x + \omega_x d_x)} F_1(\omega_x, \omega_y) \tag{3.12}$$

That means that the Fourier transform of two images differed by translation motion will have same magnitude but they are differed by phase with a phase difference which is directly related to their displacement.

If we compute cross power spectrum of the two images given by Eq-3.13 Where is F^* the complex conjugate of F.

$$\frac{F_1(\omega_x, \omega_y) F_2^*(\omega_x, \omega_y)}{\left|F_1(\omega_x, \omega_y) F_2^*(\omega_x, \omega_y)\right|} = e^{(\omega_x d_x + \omega_y d_y)} \tag{3.13}$$

So we will calculate the cross power spectrum of both the images by applying the all possible known amounts of shifts to the template, the peak of the cross power spectrum is calculated the shifts at that position is the shift between the template and image.

Since the phase difference for every frequency contributes equally, the location of the peak will not change if there is noise which is limited to a narrow bandwidth, i.e., a small range of frequencies. Thus this technique is particularly well suited to images with this type of noise. Also it is an effective technique for images obtained under differing conditions of illumination since illumination changes are usually slow varying and therefore concentrated at low-spatial frequencies.

The property of using only the phase information for correlation is sometimes referred to as a whitening of each image. Among other things, whitening is invariant to linear changes in brightness that means it is same over all parts of the image. On the other hand, if the images are affected by white noise which is spread over all frequencies then the location of the peak will be inaccurate since the phase difference at each frequency is corrupted.

Rotational movement, without translation, can be calculated in a similar manner as translation using phase correlation by representing the rotation as a translational displacement with polar coordinates. So as to register images having both shift's and rotations then we first calculate the rotation angle and the calculate shifts. Rotating an image rotates the Fourier transform of that image by the same angle. If we know the angle, then we can rotate the cross power spectrum and determine the translation according to the phase correlation method. Since we do not know the angle we compute the phase of the cross power spectrum as a function of the rotation angle estimate ϕ and use polar coordinates (r,θ) simplify the equation 3.14.

$$G(r,\theta;\phi) = \frac{F_1(r,\theta)F_2^*(r,\theta-\phi)}{\left|F_1(r,\theta)F_2^*(r,\theta-\phi)\right|} \tag{3.14}$$

Therefore, by first determining the angle θ which makes the inverse Fourier transform of the phase of the cross-power spectrum the closest approximation to an impulse, we can then determine the translation as the location of this pulse.

3.4.2.3 Point Mapping

The point or landmark mapping technique is the primary approach currently taken to register two images whose type of misalignment is unknown. This occurs if the class of transformations cannot be easily categorized such as by a set of small translations or rigid-body movements. For example, if images are taken from varying viewpoints of a scene with smooth depth variations, then the two images will differ depending on the perspective distortion. We cannot determine the proper perspective transformation because in general we do not know the actual depths in the scene, but we can use the

landmarks that can be found in both images and match them using a general transformation.

If the scene is not composed of smooth surfaces, but has large depth variations, then the distortions will include occlusions which differ between images, objects which appear in different relative positions between images, and other distortions which are significantly more local. As these distortions become more local, it will become progressively more difficult for a global point-mapping method to account for the misalignment between the images. In this case, methods which use a local transformation, Such as the local point-mapping methods, would be preferable. The general method for point mapping consists of three stages. In the first stage features in the image are computed. In the second stage, feature points in the reference image, often referred to as control points, are corresponded with feature points in the data image. In the last - stage, a spatial mapping, usually two 2D polynomial functions of a specified order (one for each coordinate in the registered image) is determined using these matched feature points. Re sampling of one image onto the other is performed by applying the spatial mapping and interpolation.

Point mapping methods are used for images whose misalignment is a small rigid or affine transformation, but which contain significant amounts of local uncorrected variations. The techniques in previous Sections are not adequate in this case because the relative measures of similarity between the possible matches become unreliable. Point mapping methods can overcome this problem by the use of feedback between the stages of finding the correspondence between control points and finding the optimal transformation.

3.5 Interpolation On To High Resolution Grid

The second step in the super resolution process is to interpolate the perfectly registered data on to a high resolution grid. A pictorial example of the overlay of three misregistered images is shown in Figure 3.4, where the sub-pixel shifts for each frame, δ_x, δ_y are also shown. Figure 3.5 shows the relationship between the subsampled, multiple low-resolution images and the high-resolution image.

The main reason that a single high-resolution frame can be constructed from low-resolution frames is that the low-resolution images are subsampled (aliased) as well as misregistered with sub-pixel shifts. If the images are shifted by integer amounts, then each image contains the same information (intensity values at the same spatial location), and thus there is no new information that can be used. In this case, a simple interpolation scheme (bilinear, cubic spline, etc.) can be used to increase the resolution. However, if the images have sub-pixel shifts, and if aliasing is present, then each image cannot be obtained from the others, assuming each image has different shifts. New information is therefore contained in each low-resolution image, and can thus be exploited to obtain a high-resolution image.

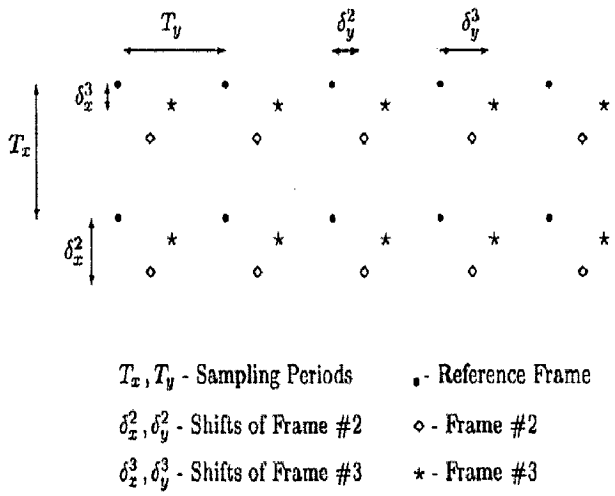

Figure 3.4 Superimposition of three misregistered images
Low resolution frames

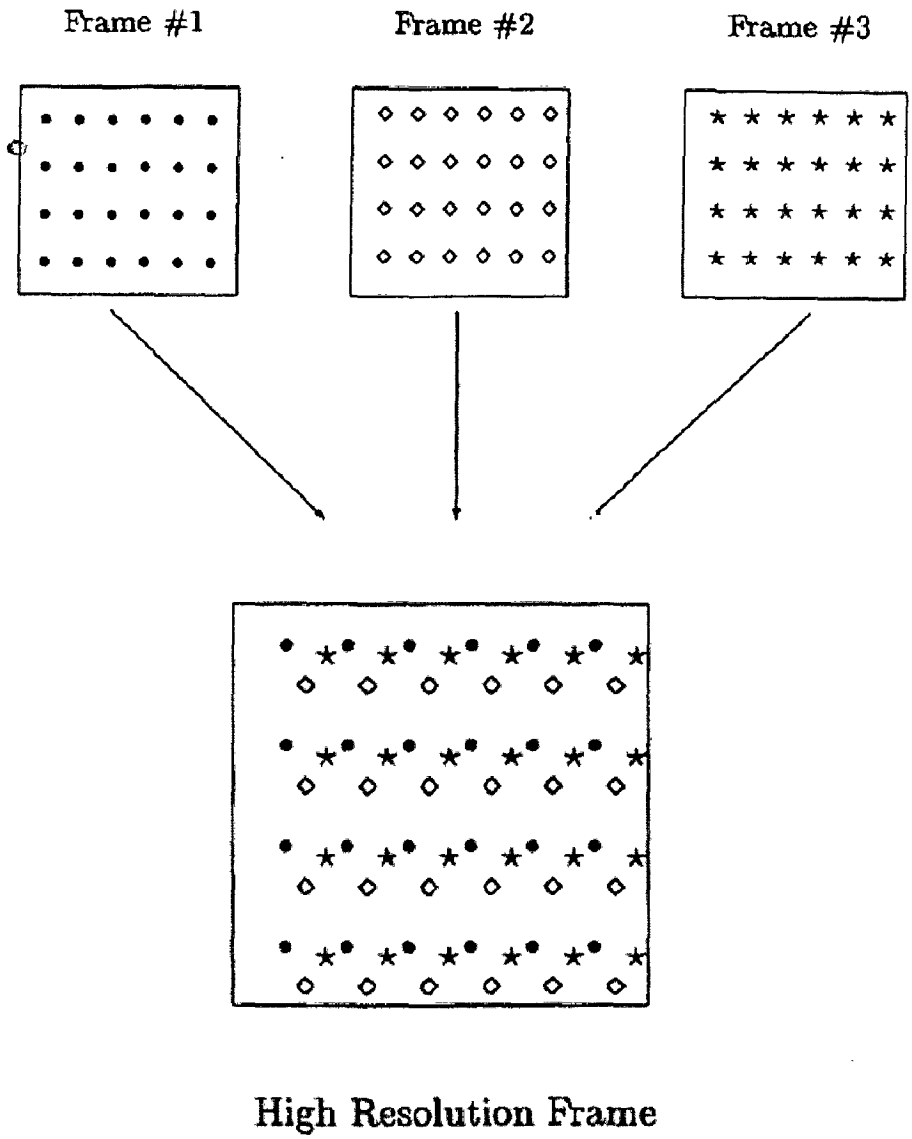

Fig 3.5 Relationship between low-resolution images and the high-resolution image

Suppose the 'k' number of low resolution images is of size 'n*n' and the resolution enhancement factor is 'r', then we have to construct a high resolution grid of size *rn*rn* from the data what we have from all these images we have to construct the pixel values at each pixel location using interpolation techniques. The type of interpolation techniques that are generally used are in image processing are discussed in

the previous chapter, along with discussion I have also discussed the advantages and disadvantages of these techniques.

Generally bi-cubic interpolation technique is used in all super resolution techniques. In the method I have implemented also I have used bi-cubic interpolation only.

3.6 Restoration for blur and noise removal

The common type of degradation that challenges the super resolution is the image blur. The process of blurring removal is called image de-blurring. Actually the blurring of image is due to capturing of images when camera or object to be captured is in motion. The amount of blurring of the image compared to the original image is governed by the PSF (point spread function). The blurring, or degradation, of an image can be caused by many factors:

- Movement during the image capture process, by the camera or, when long exposure times are used, by the subject
- Out-of-focus optics, use of a wide-angle lens, atmospheric turbulence, or a short exposure time, which reduces the number of photons captured
- Scattered light distortion in confocal microscopy.

The deblurring model:- A blurred or degraded image can be approximately described by this equation g = Hf + n, where **g the** blurred image

H The distortion operator also called the *point spread function* (PSF). In the spatial domain, the PSF describes the degree to which an optical system blurs (spreads) a point of light. The PSF is the inverse Fourier transform of the optical transfer function (OTF). In the frequency domain, the OTF describes the response of a linear, position-invariant system to an impulse. The OTF is the Fourier transform of the point spread function (PSF). The distortion operator, when convolved with the image, creates the distortion. Distortion caused by a point spread function is just one type of distortion.

the previous chapter, along with discussion I have also discussed the advantages and disadvantages of these techniques.

Generally bi-cubic interpolation technique is used in all super resolution techniques. In the method I have implemented also I have used bi-cubic interpolation only.

3.6 Restoration for blur and noise removal

The common type of degradation that challenges the super resolution is the image blur. The process of blurring removal is called image de-blurring. Actually the blurring of image is due to capturing of images when camera or object to be captured is in motion. The amount of blurring of the image compared to the original image is governed by the PSF (point spread function). The blurring, or degradation, of an image can be caused by many factors:

- Movement during the image capture process, by the camera or, when long exposure times are used, by the subject
- Out-of-focus optics, use of a wide-angle lens, atmospheric turbulence, or a short exposure time, which reduces the number of photons captured
- Scattered light distortion in confocal microscopy.

The deblurring model:- A blurred or degraded image can be approximately described by this equation g = Hf + n, where **g the** blurred image

H The distortion operator also called the *point spread function* (PSF). In the spatial domain, the PSF describes the degree to which an optical system blurs (spreads) a point of light. The PSF is the inverse Fourier transform of the optical transfer function (OTF). In the frequency domain, the OTF describes the response of a linear, position-invariant system to an impulse. The OTF is the Fourier transform of the point spread function (PSF). The distortion operator, when convolved with the image, creates the distortion. Distortion caused by a point spread function is just one type of distortion.

F The original true image

N Additive noise, introduced during image acquisition, that corrupts the image

Apart from the deblurring of the image there may be several kinds of noises may be present in the images depending on the atmospheric conditions and type of images to be captured and all. Depending on the type of noise we have to use certain noise removal algorithms. These techniques may be in spatial domain or in frequency domain. We have to select the noise removal phenomenon depending on the type of noise present in the image. Also in super resolution imaging some times shot noise may be come in to picture because of misregistration of images, which can be come in to picture because of errors in the registration algorithms.

3.7 Conclusion

Relation between high resolution image and low resolution image is Cleary explained using block diagram. Generalized block diagram of super resolution scheme is shown and each block is discussed clearly. The significance of registration in super resolution is explained and different image registration techniques are described and explained related to computational time and application. It has been found that normal correlation techniques are easy to understand but their computational time is maximum. Interpolation on to high resolution grid after registering the LR images is clearly explained.

CHAPTER 4

Modified Frequency Domain Approach to Super Resolution

4.1 Introduction

In the previous chapters we have discussed the basic interpolation techniques and their advantages and disadvantages. It has also been discussed tat the usefulness of super resolution. Also we have discussed the basic steps included in the basic super resolution achievement scheme. In the third chapter discussion has gone through the importance of registration in super resolution, also it covers the other blocks present in the super resolution scheme like interpolation on to high resolution grid and post processing techniques like blur removal and other types of noise removal schemes. All the discussion in the previous chapters is quite useful in this chapter to construct a HR frame from set of LR frames.

This chapter covers the explanation about the reconstruction of HR frame by using a special frequency domain technique specially suited for input images of type aliased and misregistered. The resulting image is aliasing-free. A small aliasing-free part of the frequency domain of the images is used to compute the exact subpixel shifts. This algorithm is best suited for images which are affected by noise because for registration we are going to construct the low frequency information for registering the images.

4.2 Concept of shifting in the images

The block registration covers the process of finding the shift and rotation parameters between the images. The first image is taken as the reference image and other images are called templates. In the modified frequency domain algorithm considers the number of LR input images as 4. Then first image is called as reference image and other 3 are template images. As we have already considered the statement that the images are subsampled and aliased. So firstly we will go through the shift estimation in one dimension as in [5].

4.2.1 Concept of Shift in One Dimension

The $s(t)$ is a band limited continuous signal with maximal frequency f_{max}. This signal is sampled at times $t_0, t_0+T, t_0+2T.....,t_0+NT$ with a sampling frequency f_s, taking $f_s > f_{max}$. This result in a sampled signal $s_1[n]$, n = 0, 1... N. We now sample $s(t)$ again, at the same sampling frequency f_s, but at times $t_0+\delta, t_0+T+\delta, t_0+2T+\delta.....,t_0+NT+\delta$, which are shifted by an unknown shift δ compared to the first set of sampling times. We call this sampled signal $s_2[n]$, n = 0, 1... N. This is shown in the figure 4.1.

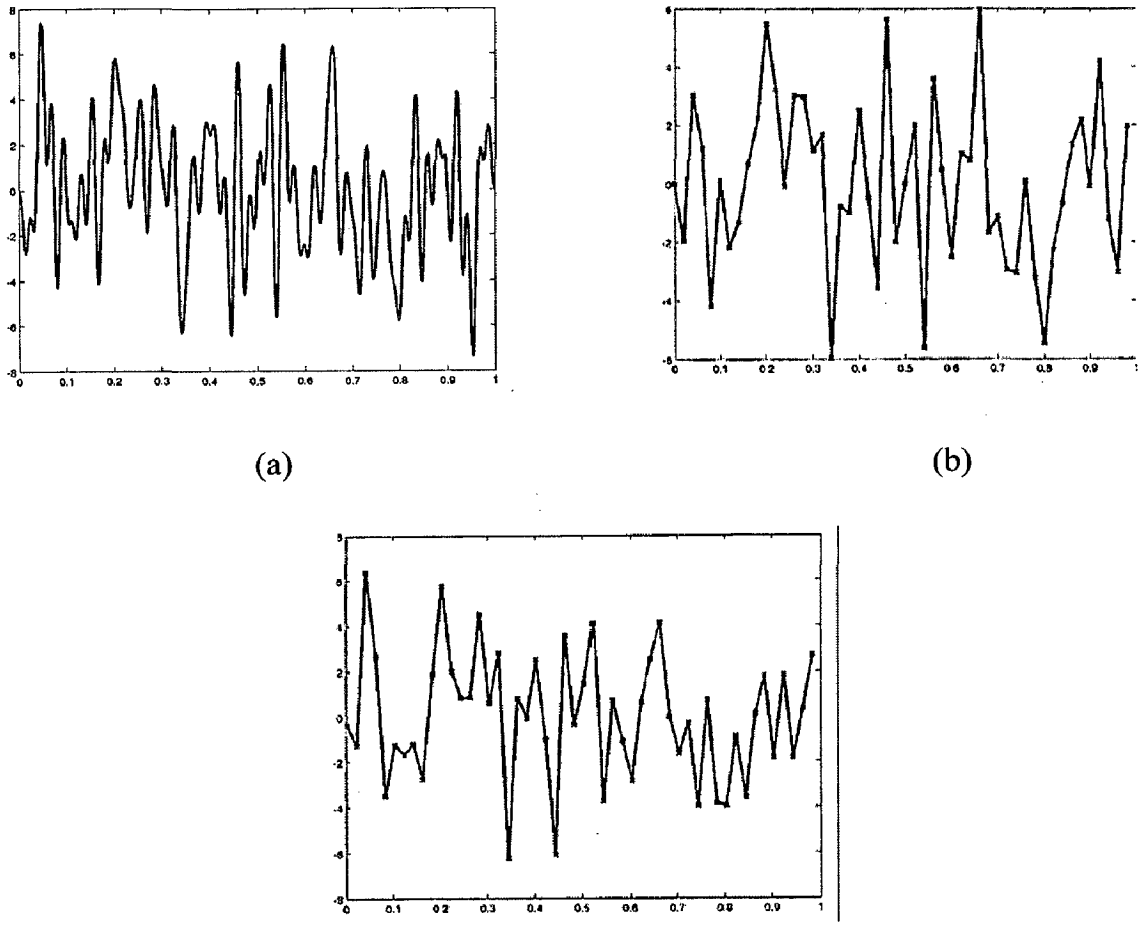

(a) (b)

(c)

Figure 4.1. (a) Original signal $s(t)$. (b) And (c) Sampled and aliased signals $s_1[n]$ and $s_2[n]$.[5]

If f_s satisfies the Nyquist criterion, $f_s > 2f_{\max}$, s(t) can be perfectly reconstructed from $s_1[n]$or $s_2[n]$ separately, and the shift δ - although not needed because $s(t)$ has already been reconstructed - can be derived from the two reconstructions using a correlation operator. One signal is sufficient to make a perfect signal reconstruction.

If we assume f_s has a value $f_{\max} < f_s < 2f_{\max}$, we know from Shannon sampling theory that a perfect reconstruction of $s(t)$ from $s_1[n]$or $s_2[n]$ is not possible, because $s_1[n]$ and $s_2[n]$ will be aliased. Direct computation of δ using a correlation operator is impossible, because the aliasing effect causes the two signals to be different.

But because $f_{\max} < f_s$, $s_1[n]$and $s_2[n]$ also have a part that is aliasing-free, namely for the frequencies $|f| < f_s - f_{\max}$. It is then possible to apply a low pass filter to $s_1[n]$ and $s_2[n]$ with cutoff frequency $f_s - f_{\max}$, which results in two identical, aliasing-free signals $s_{1,low}[n]$ and $s_{2,low}[n]$ (Figure 2). If suppose $s(t)$ has non-zero energy in the frequency band $-f_s + f_{\max} < f < f_s - f_{\max}$, δ can be computed from $s_{1,low}[n]$ and $s_{2,low}[n]$ using a correlation operation.

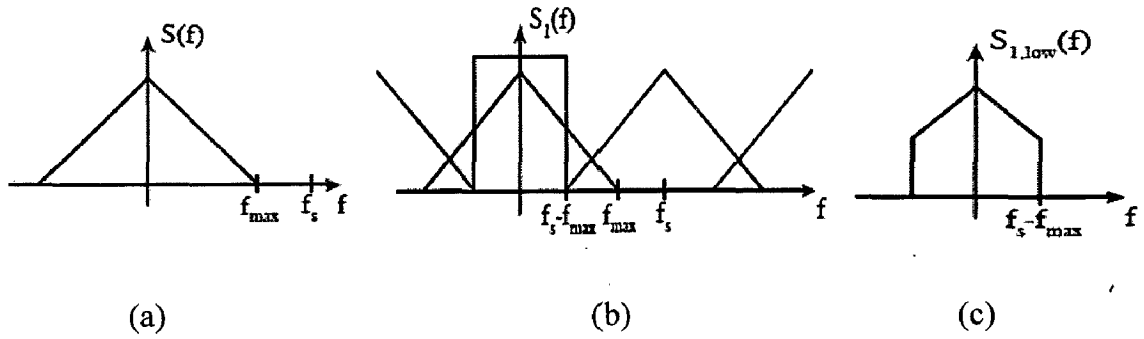

Figure 4.2 (ref [5]) (a) Original signals $s(t)$. (b) Sampled and aliased signal $s_1[n]$ with the appropriate low pass filter indicated. (c) Low pass filtered signal $s_{1,low}[n]$

4.2.2 Concept of shift in 2D

This method can now easily be generalized to two-dimensional signals by performing all operations on the two signal dimensions (rows and columns) separately. We start from a 2D signal r(x, y), which has maximal horizontal frequency $f_{c,v} = f_{s,v} - f_{\max,v}$ and vertical frequency $f_{\max,v}$ Sampling at

$$\begin{bmatrix} (x_0, y_0) & (x_0 + T_x, y_0) & (x_0 + 2T_x, y_0) & \dots & (x_0 + MT_x, y_0) \\ (x_0, y_0 + T_y) & (x_0 + T_x +, y_0 + T_y) & (x_0 + 2T_x +, y_0 + T_y) & : & (x_0 + MT_x +, y_0 + T_y) \\ : & : & : & : & : \\ : & : & : & : & : \\ (x_0, y_0 + NT_y) & x_0 + T_x +, y_0 + NT_y & x_0 + 2T_x +, y_0 + NT_y & \dots & x_0 + MT_x +, y_0 + NT_y \end{bmatrix} \quad (4.1)$$

For $r_1[k,l]$ and at

$$\begin{bmatrix} (x_0+\delta_x, y_0+\delta_y) & (x_0+\delta_x+T_x, y_0+\delta_y) & (x_0+\delta_x+2T_x, y_0) & \dots & (x_0+\delta_x+MT_x, y_0+\delta_y) \\ (x_0+\delta_x, y_0+T_y) & (x_0+\delta_x+T_x+, y_0+\delta_y+T_y) & (x_0+\delta_x+2T_x+, y_0+T_y) & : & (x_0+\delta_x+MT_x+, y_0+\delta_y+T_y) \\ : & : & : & : & : \\ : & : & : & : & : \\ (x_0+\delta_x, y_0+\delta_y+NT_y) & x_0+\delta_x+T_x+, y_0+\delta_y+NT_y & x_0+\delta_x+2T_x+, y_0+NT_y & \dots & x_0+\delta_x+MT_x+, y_0+\delta_y+NT_y \end{bmatrix} \quad (4.2)$$

For $r_2[k,l]$, the signal is sampled twice, with horizontal and vertical sampling frequencies $f_{\max,h} < f_{s,v} < 2f_{\max,h}$ and $f_{\max,v} < f_{s,v} < 2f_{\max,v}$. T_x and T_y are the horizontal and vertical sampling periods, respectively. This results again in two aliased signals, which can then be low pass filtered to $r_{1,low}[k,l]$ and $r_{2,low}[k,l]$ (with filters having cutoff frequencies $f_{c,h} = f_{s,h} - f_{\max,h}$ and $f_{c,v} = f_{s,v} - f_{\max,v}$).

4.3 Motion Estimation

Here in this implementation we use modified frequency domain algorithm to estimate the motion parameters between the reference image and each of the other images. In this method we will deal with only planar motion which means that motion is allowed parallel to the image plane. That means that zooming of the camera for taking templates is not allowed[6]. The motion can be described as a function of three

parameters: horizontal and vertical shifts, Δx1 and Δx2, and a planar rotation angle ϕ. In this method we try to estimate the rotation first and then after compensation try to estimate the shifts along x and y directions.

Suppose the $f_1(x)$ is the reference image and $f_2(x)$ is the shifted and rotated version of $f_1(x)$

$$f_2(x) = f_1(R(x+\Delta x)) \tag{4.3}$$

Where

$$x = \begin{bmatrix} x_1 \\ x_2 \end{bmatrix}, \Delta x = \begin{bmatrix} \Delta x_2 \\ \Delta x_2 \end{bmatrix}, R = \begin{bmatrix} \cos\phi & -\sin\phi \\ \sin\phi & \cos\phi \end{bmatrix}$$

Suppose if we apply Fourier transform for equation (4.3) the same equation can be expressed in Fourier domain as

$$\begin{aligned} F_2(u) &= \iint_x f_2(x) e^{-j2\pi u^T x dx} \\ &= \iint_x f_1(R(x+\Delta x)) e^{-j2\pi u^T x} dx \\ &= e^{j2\pi u^T \Delta x} \iint_{x'} f_1(R(x')) e^{-j2\pi u^T x'} dx' \end{aligned} \tag{4.4}$$

Where $F_2(u)$ is Fourier transform of $f_2(x)$ and co-ordinate transform transformation $x' = x + \Delta x$. After transformation $x'' = Rx'$ the relation between the amplitudes of the Fourier transforms can be computed as

$$\begin{aligned} |F_2(u)| &= \left| e^{j2\pi u^T \Delta x} \iint_x f_2(x) e^{-j2\pi u^T x'} dx' \right| \\ &= \left| \iint_{x'} f_1(Rx') e^{-j2\pi u^T x'} dx' \right| \\ &= \left| \iint_{x'} f_1(x'') e^{-j2\pi u^T (R^T x'')} dx'' \right| \\ &= \left| \iint_{x''} f_1(x'') e^{-j2\pi (Ru)^T x'')} dx'' \right| \\ &= |F_1(Ru)| \end{aligned} \tag{4.5}$$

Where $F_2(u)$ is the shifted and rotated version of $F_1(u)$ over the same angle ϕ as the spatial domain rotation, this is shown in the figure 4.3 $|F_1(u)|$ and $||F_2(u)|$ do not depend on the shift values Δx, because the spatial domain shifts only affect the phase values of the Fourier transforms.

Therefore we can first estimate the rotation angle θ from the amplitudes of the Fourier transforms $|F_1(u)|$ and $||F_2(u)|$. After compensation for the rotation, the shift Δx can be computed from the phase difference between $F_1(u)$ and $F_2(u)$.

4.3.1 Rotation estimation

The rotation angle between $|F_1(u)|$ and $|F_2(u)|$ can be computed as the angle θ for which the Fourier transform of the reference image $|F_1(u)|$ and the rotated Fourier transform of the image to be registered $|F_2(R_\theta u)|$ have maximum correlation. That means that we have to calculate the correlation between $|F_1(u)|$ and $|F_2(u)|$ after rotating $|F_2(u)|$ for every angle and note the angle where the correlation is maximum. But this method is computationally in sensitive and also not precise.

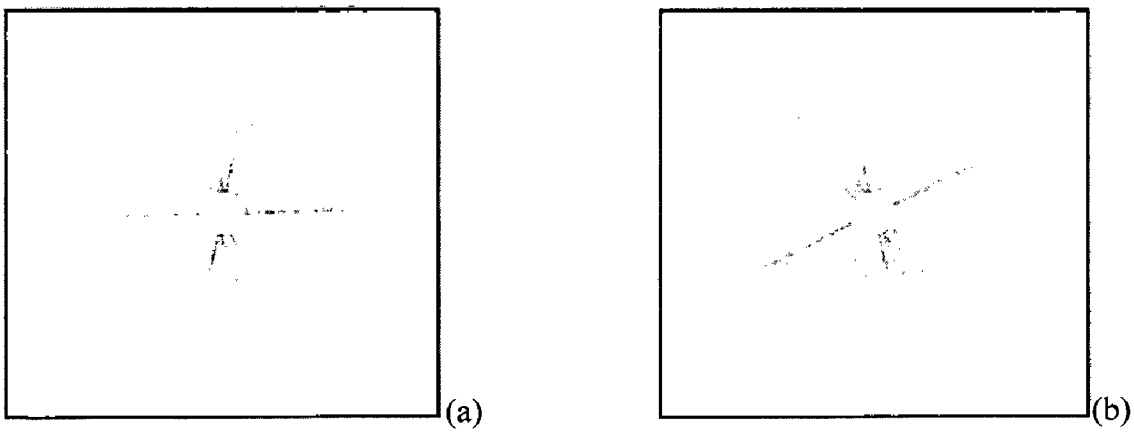

Fig 4.3 (a) Fourier transform of reference image $|F_1(u)|$, (b) of template image $|F_2(u)|$

This modified frequency domain method will first compute the frequency content h as a function of α by integrating over radial lines

$$h(\alpha) = \int_{\alpha-\Delta\alpha/2}^{\alpha+\Delta\alpha/2} \int_{0}^{\infty} |F(r,\theta)| dr d\theta \tag{4.6}$$

$|F(r,\theta)|$ Is a discrete signal. Therefore, we compute the discrete function $h(\alpha)$ as the average of the values on the rectangular grid that have an angle $\alpha - \Delta\alpha/2 < \theta < \alpha + \Delta\alpha/2$.

Suppose if we want to compute the rotation angle with a precision of 0.1 degrees, $h(\alpha)$ is computed for every 0.1 degrees.

Since $F(r,\theta)$ is a rectangular grid the value of r will be different for different values of α. To get a similar number of signal values $|F(r,\theta)|$ at every angle, the average is calculated on a circular disc of values for which $r < \rho$ (where ρ is the image radius or half the image size).

Also since the values for low frequencies are very large compared to the other values and are very coarsely sampled as a function of the angle, so we ignore the values for which $r < \varepsilon\rho$, with $\varepsilon = 0.1$. Thus, $h(\alpha)$ is computed as the average of the frequency values on a discrete grid with $\alpha - \Delta\alpha/2 < \theta < \alpha + \Delta\alpha/2$ and $\varepsilon\rho < r < \rho$.

The functional value of $h(\alpha)$ for both $|F_1(u)|$ and $|F_2(u)|$. The exact rotation angle can then be computed as the value for which their correlation reaches a maximum. This tells the great advantage of this method, that is it is using one dimensional correlation compared to conventional methods. Because of this the computational complexity of this method is drastically decreased compared to other methods.

4.3.2 Shift Estimation

A shift of the image parallel to the image plane (planar motion) can be expressed in Fourier domain as a linear phase shift:

$$F_2(u) = \iint_x f_2(x) e^{-j2\pi u^T x} dx = \iint_x f_1(x+\Delta x) e^{-j2\pi u^T x dx} \tag{4.7}$$

$$= e^{j2\pi u^T \Delta x} \iint_x f_1(x') e^{-j2\pi u^T x'} dx' = e^{j2\pi u^T \Delta x} F_1(u)$$

So to find the shift parameters Δx we have to compute the slope of the phase difference $-u_s + u_{\max} < u < u_s - u_{\max}$. This will give the number of values equal to the size of the Fourier transform of the image so we will take the least square solution of all the values and that will be the phase difference from which we can easily calculate the shift parameters.

4.4 Considerations to Be Taken If the Input Images Are Aliased

Because the images are aliased the concept of the shift and rotation estimation that are used above by it self won't give precise registration. But the above concept with certain amount of changes is used to achieve precise registration.

The shift estimation equation described above can be expressed as with sampling u_s frequency of and $2K+1$ overlapping spectrum copies at frequency $\boldsymbol{u}$.

$$F_2(u) = \sum_{k=-K}^{K} e^{j2\pi(u-ku_s)\Delta x} F_1(u - ku_s) \tag{4.8}$$

Because of the aliasing the linear relation between $F_1(u)$ and $F_2(u)$ is disturbed. First the signals $f_1[k]$ and $f_2[k]$ are first low-pass filtered (with cutoff frequency which is difference of sampling frequency of images and the maximum frequency of input image) in horizontal and vertical dimensions.

Since motion and rotation estimation algorithms work in frequency domain we can just take the low frequency part to work out the shift and rotation estimation. The rotation estimation is done for the frequencies for which $\varepsilon\rho < r < \rho_{\max}$ (with $\rho_{\max=} \min(u_s - u_{\max})/u_s$), and the horizontal and vertical shifts are estimated from the phase differences for $-u_s + u_{\max} < u < u_s - u_{\max}$

4.5 Practical implementation

The algorithm for practical implementation is shown in the figure 4.4.

- First set of misregistered and aliased low resolution images $f_{LR,m}$ are taken.
- Multiply these images by Tukey window to make them circularly symmetric. Circularly symmetric signals[7],[8] :-

  An arbitrary 2D signal $a(x, y)$ can always be written in a polar coordinate system as $a(r, \theta)$. When the 2D signal exhibits a circular symmetry this means that:

$$a(x, y) = a(r, \theta) = a(r) \tag{4.9}$$

Where $r^2 = x^2 + y^2$ and $\tan\theta = y/x$. As a number of physical systems such as lenses exhibit circular symmetry, it is useful to be able to compute an appropriate Fourier representation.

If the images are color each image consists of red, green and blue parts. So we can not directly pass these images directly to shift and rotation estimation functions. So we will first separate these three parts and we will pass one of these to the estimation algorithms. The shift and rotation will be same for all these three components. So after getting the shift and rotation parameters again all three components are added to obtain a RGB (colored) image.

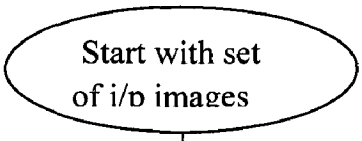

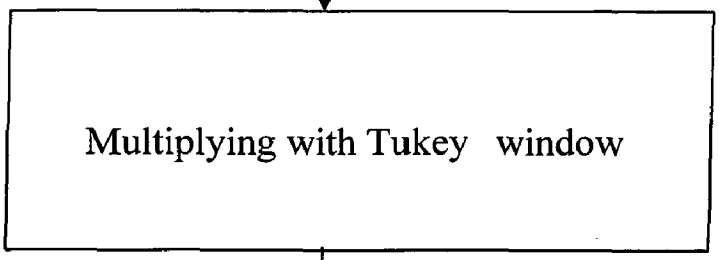

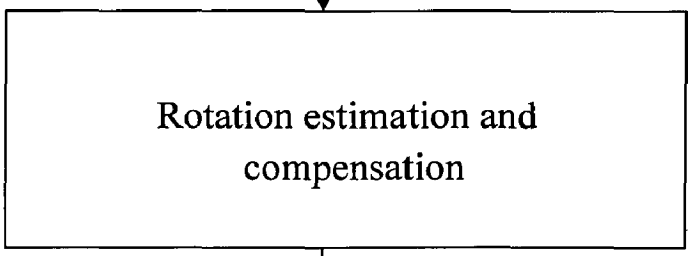

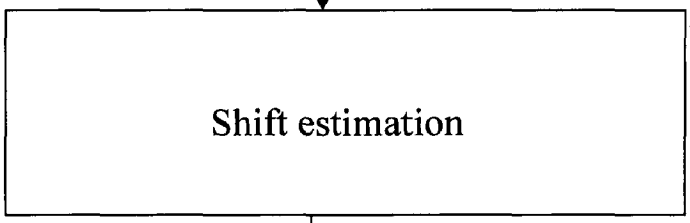

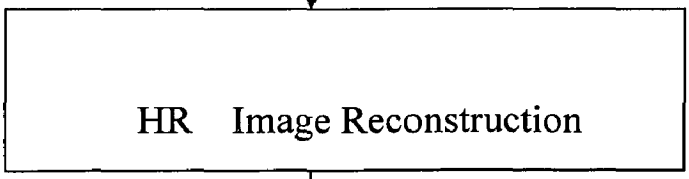

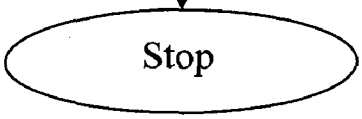

Fig 4.4 Flow Chart Of Practical Implementation

- Rotation estimation: The rotation angle between every image $f_{LR,w,m}(m=2,...,M)$ and the reference image $f_{LR,w,1}$ is estimated.
  a) Compute the polar coordinates (r,θ) of the image samples.
  b) For every angle α, compute the average value $h_m(\alpha)$ of the Fourier coefficients for which $\alpha-1<\theta<\alpha+1$ and $0.1\rho<r<\rho_{\max}$. The angles are expressed in degrees and $h_m(\alpha)$ is evaluated every 0.1 degrees. A typical value used for $\rho_{\max}$ is 0.6.
  c) Find the maximum of the correlation between $h_1(\alpha)$ and $h_m(\alpha)$ between -30 and 30 degrees. This is the estimated rotation angle ϕ_m.
  d) Rotate image $f_{LR,w,m}$ by $-\phi_m$ to cancel the rotation.

- Shift estimation: the horizontal and vertical shifts between every image $f_{LR,w,m}(m=2,...,M)$ and the reference image $f_{LR,w,1}$ are estimated.
  a) Compute the phase difference between image m and the reference image as $\angle(F_{LR,w,m}/F_{LR,w,1})$.
  b) For all frequencies $-u_s+u_{\max}<u<u_s-u_{\max}$ write the linear equation describing a plane through the computed phase difference with unknown slopes Δx.
  c) Find the shift parameters Δx_m as the least squares solution of the equations.

- Image reconstruction: a high-resolution image f_{HR} is reconstructed from the registered images $f_{LR,m}(m=1,...,M)$.
  a) For every image $f_{LR,m}$, compute the coordinates of its pixels in the coordinate frame of $f_{LR,1}$ using the estimated registration parameters.
  b) From these known samples, interpolate the values on a regular high-resolution grid using for example cubic interpolation.

4.6 Reconstruction

When the low-resolution images are accurately registered, the samples of the different images can be combined to reconstruct a high-resolution image. For this the interpolation techniques discussed in the previous chapters are used. In this reconstruction algorithm, the samples of the different low-resolution images are first expressed in the coordinate frame of the reference image. Then, based on these known samples, the image values are interpolated on a regular high-resolution grid. Here in this technique bicubic interpolation is choosing because of its low computational complexity and good results.

4.7 Conclusion

Modified frequency domain technique for image registration technique has been well explained. This method uses one dimensional correlation in rotation estimation while other methods use two dimensional correlations. So obviously the time complexity of rotation estimation algorithm will be less. Also the time complexity for shift estimation algorithm is also less since it uses least square solution method rather than finding correlation for different shifts. So in this method correlations are avoided in shift estimation and it reduced to one dimensional correlation in rotation estimation.

Since low frequency part of the images is used for registration algorithms the problems of aliasing will not come in to picture. So this technique is best suited for images affected by aliasing.

CHAPTER 5
RESULTS AND DISCUSSION

5.1 Introduction

The algorithm presented in this thesis uses a set of 4 low resolution frames to construct a single high resolution image. The images are aliased and misregistered. So as to capture these set of LR images we will put camera on a tripod and we will take one image. After a small unknown amount of displacement, rotation is applied to the camera and again another image. This process is repeated for another two times to capture another two images. The images are numbered $im(1), im(2), im(3)$ and $im(4)$. The first image is called reference image and all three images are named as template images. Along with the LR (low resolution images) a high resolution image is also taken by a camera with a double resolution.

Form these input images HR image is constructed by the explained modified frequency domain algorithm and also by the basic interpolation techniques which uses a single image. All HR images constructed from the algorithms are compared with the original image to calculate the mean error. im_r Is the reconstructed image from the Frequency domain multiple frame super resolution algorithms, im_{bc} is the result of bicubic interpolation, im_{bl} is the result of bilinear interpolation and im_{nr} is the result of nearest neighborhood interpolation. im_h Is the original high resolution image and im_r is the constructed image form the Multiframes approach. Suppose size of the LR frames is M x M then size of HR frame would be 2M x 2M.

The error function is given by the formulation

$$E = \sqrt{\sum_{i=0}^{2M}\sum_{j=0}^{2M}\left(im(i,j) - im_h(i,j)\right)^2 / \left(\sum_{i=0}^{2M}\sum_{j=0}^{2M} im_h(i,j)/4M^2\right)} \qquad (5.1)$$

The error function is the square root of the sum of the differences of squares of the pixel to pixel intensities of original image to the constructed image divided by the average pixel intensity of the original image.

The constructed HR image by the modified frequency domain Multiframes approach will be a little shifted and rotated version of the image that is taken originally by a high resolution camera, since this has been constructed form set of images. In this case whenever we are taking the pixel to pixel difference it should be remembered that we are taking the difference between pixels at different locations. So as to compensate for these shifts first the motion parameters between the original and the resultant image are calculated and compensation for shift is given to the resultant image. In this case value of the error function improves compared to conventional methods. In the present work study has been done on 15 sets of images. It has been found that the value of error function decreases by an amount of 40-50 percent compared to conventional interpolation techniques.

Among the studies datasets some of them are shown in the later pages.

5.2 Dataset 1

A set of four low resolution images are taken for a constructed wall by taking the considerations explained above. Canon PowerShot A460 camera is used for this dataset. The low resolution frames are taken by keeping picture size at 640*480. When ever we keep picture size like this some of the photo detectors in the camera will be inactive. For example in a horizontal direction photo detector array photo detector 1 will be active and photo detector 2, 3, 4 will be inactive again photo detector 5 will be active. So we will be able o achieve a low resolution image. At the same instant another image of the same scene wit double resolution is also taken at a picture size of 1280*960.

This image is not having many variations through out it. Results of dataset are shown by the figure 5.1. In this figure (a), (b), (c), (d) are the set of misregistered and aliased images. Figure 5.1 (f) is the output of nearest neighborhood interpolation to double its resolution which uses only image $im(1)$ shown in figure 5.1(a) as input. Similarly figure 5.1(g), 5.1(h) are the outputs of bilinear and bicubic interpolations.

Finally figure 5.1(i) is the high resolution image from the multiframe modified frequency domain method and 5.1(j) is the original high resolution image directly taken from high resolution camera.

It has been found that the nearest neighbor hood interpolation producing an image having blocky appearance at some parts of the image. And linear interpolation is creating an output image affected by blur. Bicubic interpolation is producing a comparable picture with the high resolution image but still it is producing a considerable blur at high frequency edges.

Output of multiframe method is producing a good comparable image with the original high resolution image which is better than all the conventional interpolation techniques. The shift parameters between the low resolution images and the error functions of the constructed HR images with the original image are calculated and tabled in table 5.1 and 5.2.

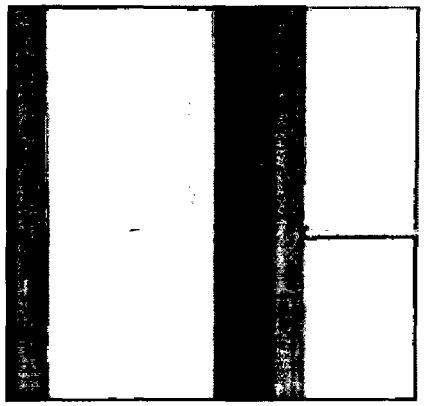

(a) LR frame 1 *im*(1)

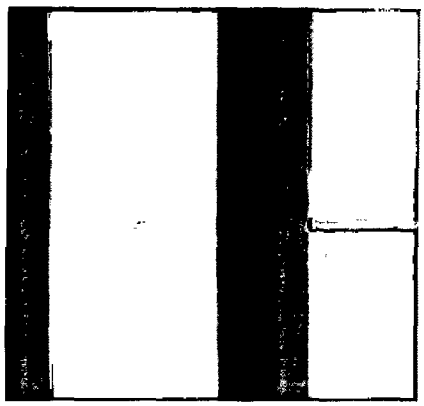

(b) LR frame 2 *im*(2)

(c) LR frame 3 *im*(3)

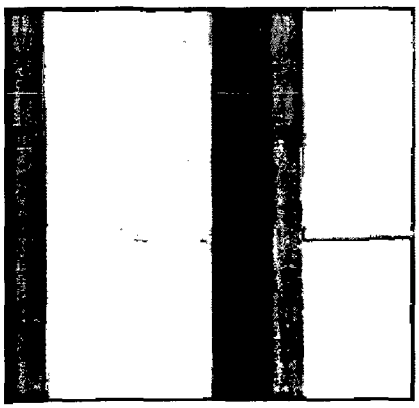

(d) LR fame 4 *im*(4)

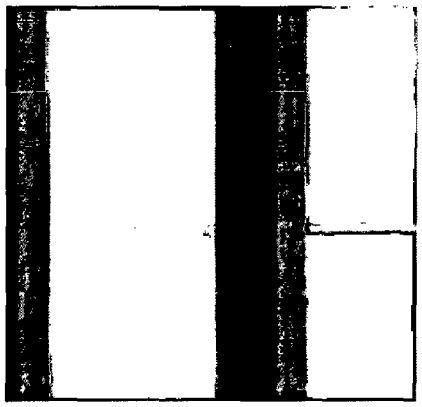

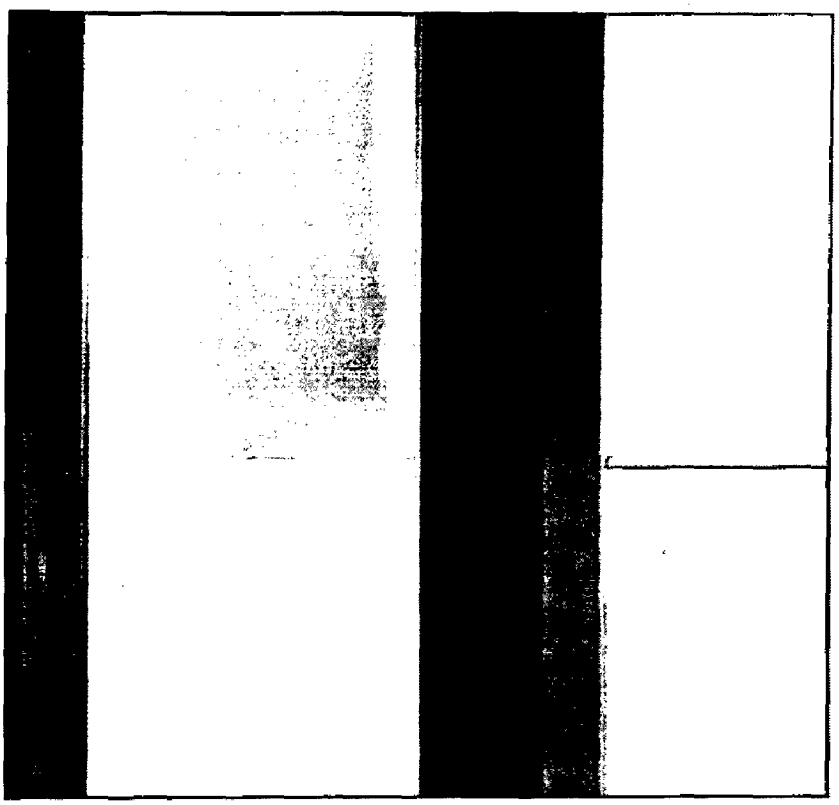

(e) O/P Nearest Neighborhood Interpolation

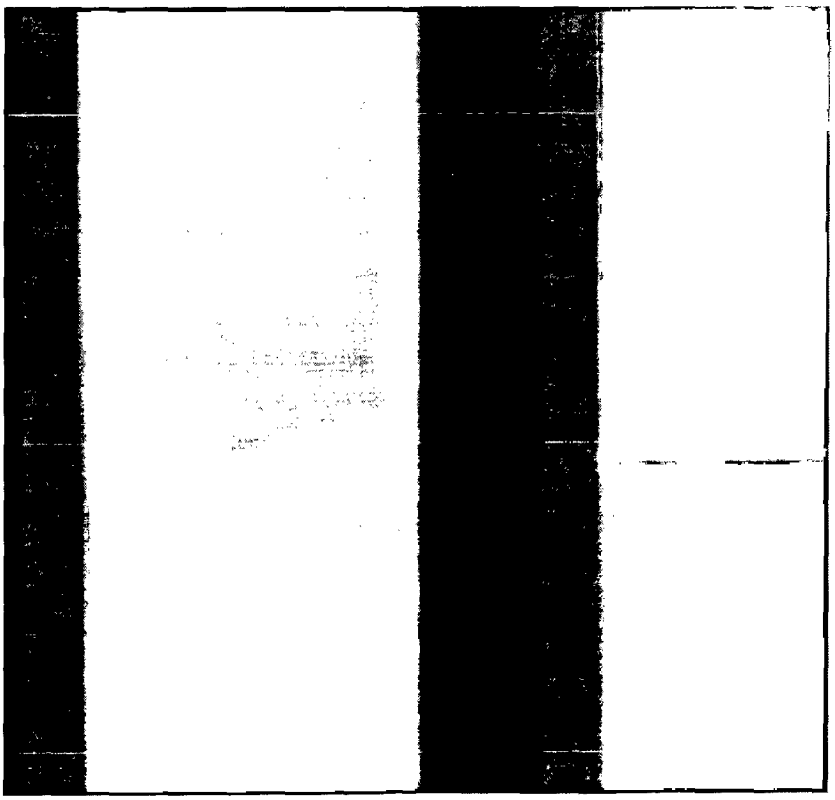

(f) O/P of Bilinear Interpolation

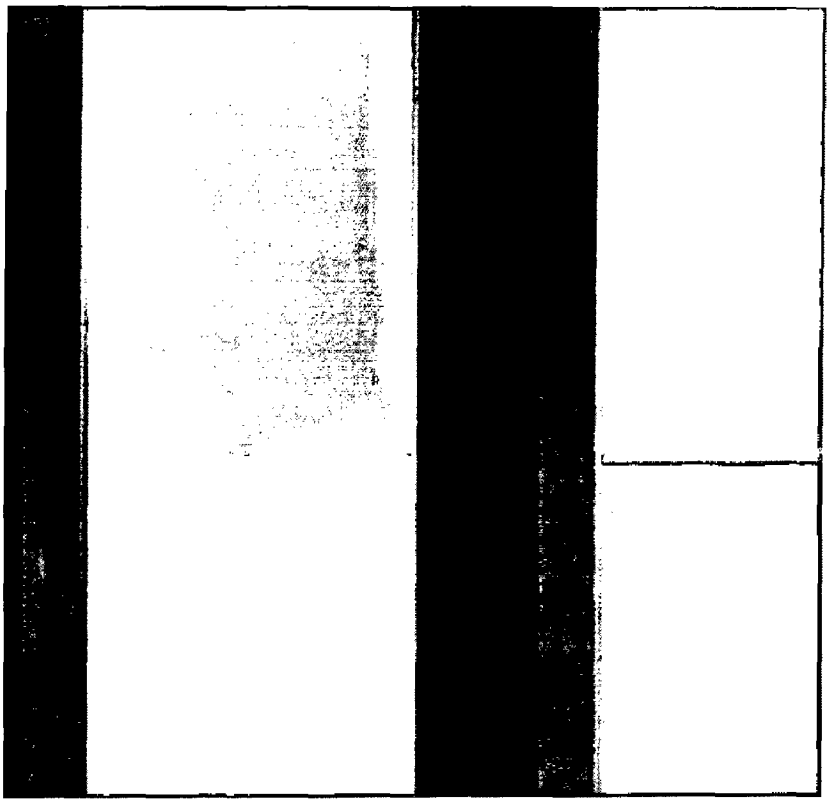

(g) O/P of Bicubic Interpolation

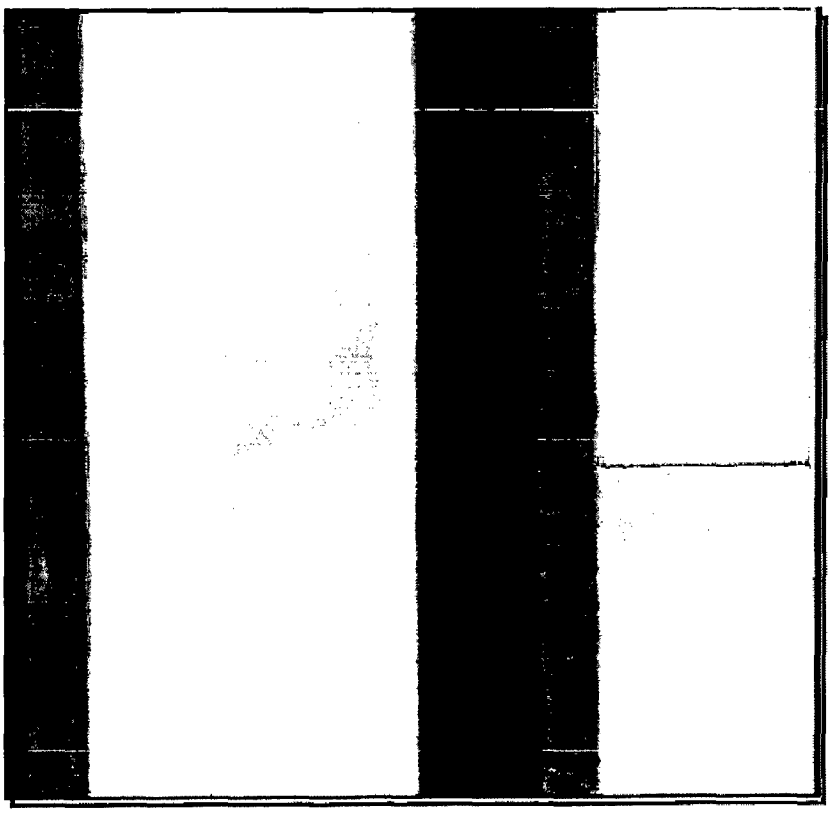

(h) O/P of Frequency domain Multiframes algorithm

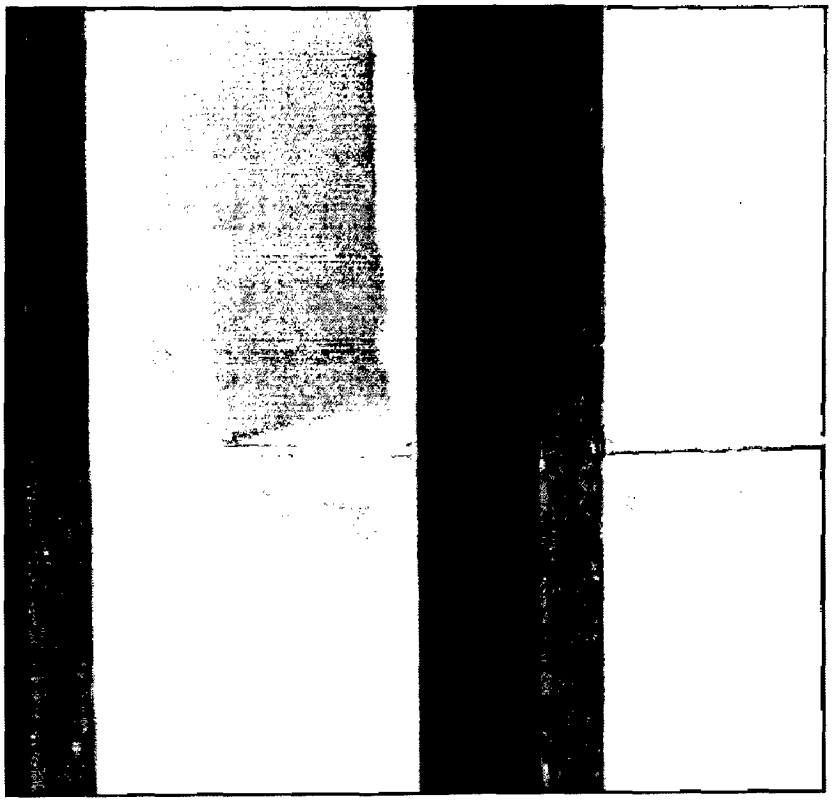

(i) Original Image

Figure 5.1 (a), (b), (c), (d) set of low resolution images

(e) ---- Output of nearest neighbor interpolation

(f)----- Output of bilinear interpolation

(g)-----Output of bicubic interpolation

(h)--- Output of modified frequency domain approach

(i)---- Original high resolution image.

Motion Parameters

	Shift parameters		Rotation parameter
LR frames	Δx	Δy	θ
im(1)	**0**	**0**	**0**
im(2)	**1.6828**	**-0.2699**	**-0.1000**
im(3)	**-0.4756**	**-0.1488**	**-0.1000**
im(4)	**0.7924**	**-0.2115**	**-0.1000**

Table 5.1

Error comparison

Type of technique	**Nearest neighbor**	**Bilinear interpolation**	**Bicubic interpolation**	**Implemented algorithm**
Error	**0.0735**	**0.0655**	**0.0735**	**0.04789**

Table 5.2

The shifts between the images are small and the rotation is negligible. The shifts are in terms of subpixel shifts of low resolution images. Since the shifts are evenly distributed over the 0-1 scale we can expect a good image form the multiframe method. The error comparison table also suggests that. The error of the multiframe method is 35 percent less than the conventional bicubic interpolation method.

5.3 Dataset 2

A set of four low resolution images are taken for a constructed wall by taking the considerations explained above. Nikon Coolpix 5600'scamera is used for this dataset. The low resolution frames are taken by keeping picture size at 640*480. When ever we keep picture size like this some of the photo detectors in the camera will be inactive. For example in a horizontal direction photo detector array photo detector 1 will be active and photo detector 2, 3, 4 will be inactive again photo detector 5 will be active. So we will be able o achieve a low resolution image. At the same instant another image of the same scene wit double resolution is also taken at a picture size of 1280*960.

This image is not having many variations through out it. Results of dataset are shown by the figure 5.2. In this figure (a), (b), (c), (d) are the set of misregistered and aliased images. Figure 5.2 (f) is the output of nearest neighborhood interpolation to double its resolution which uses only image $im(1)$ shown in figure 5.2(a) as input. Similarly figure 5.2(g), 5.2(h) are the outputs of bilinear and bicubic interpolations.

Finally figure 5.2(i) is the high resolution image from the multiframe modified frequency domain method and 5.2(j) is the original high resolution image directly taken from high resolution camera.

It has been found that the nearest neighbor hood interpolation producing an image having blocky appearance at some parts of the image. And linear interpolation is creating an output image affected by blur. Bicubic interpolation is producing a comparable picture with the high resolution image but still it is producing a considerable blur at high frequency edges.

Output of multiframe method is producing a good comparable image with the original high resolution image which is better than all the conventional interpolation techniques. The shift parameters between the low resolution images and the error functions of the constructed HR images with the original image are calculated and tabled in table 5.3 and 5.4.

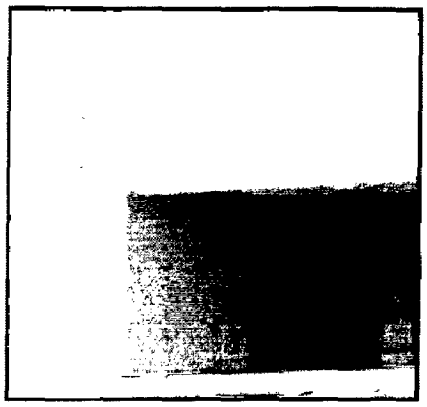

(a)LR frame 1 *im*(1)

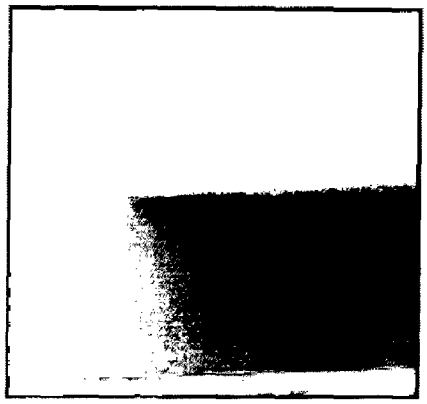

(b)LR frame 2 *im*(2)

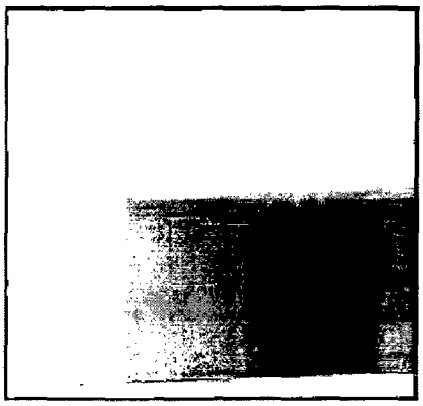

(c) LR frame 3 *im*(3)

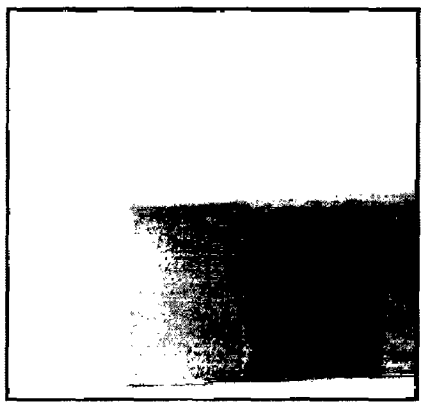

(d) LR frame 4 *im*(4)

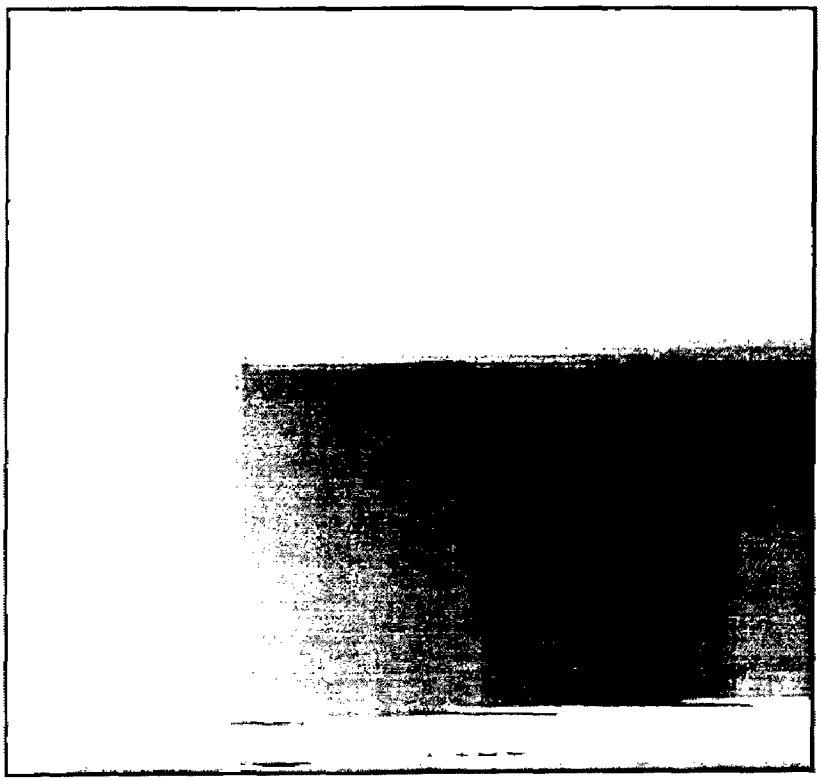

(e) O/P of nearest neighbor interpolation

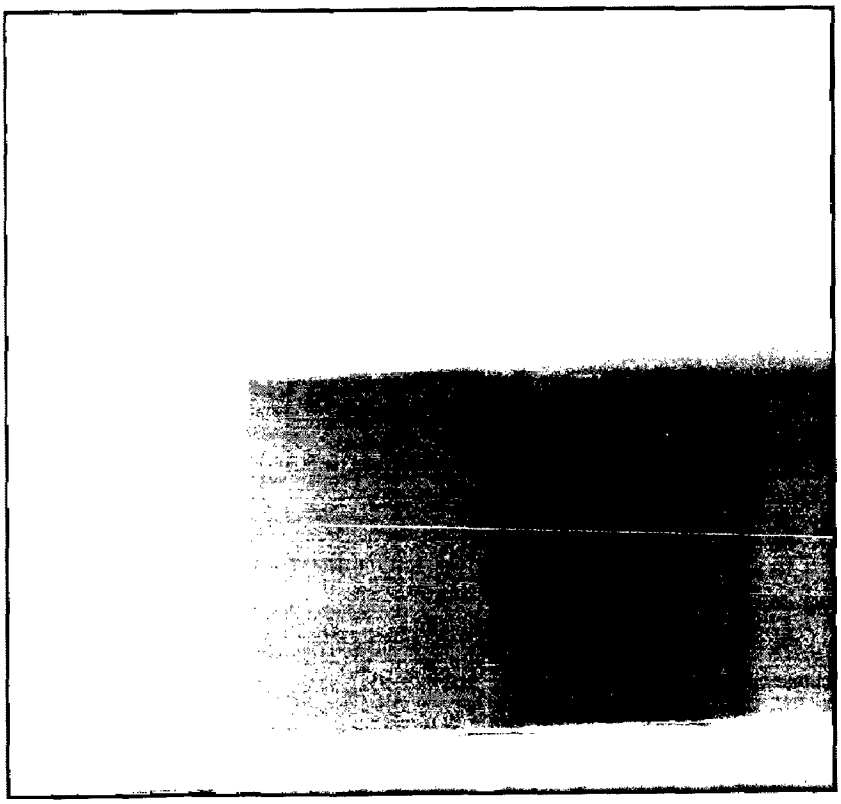

(f) Bilinear interpolation

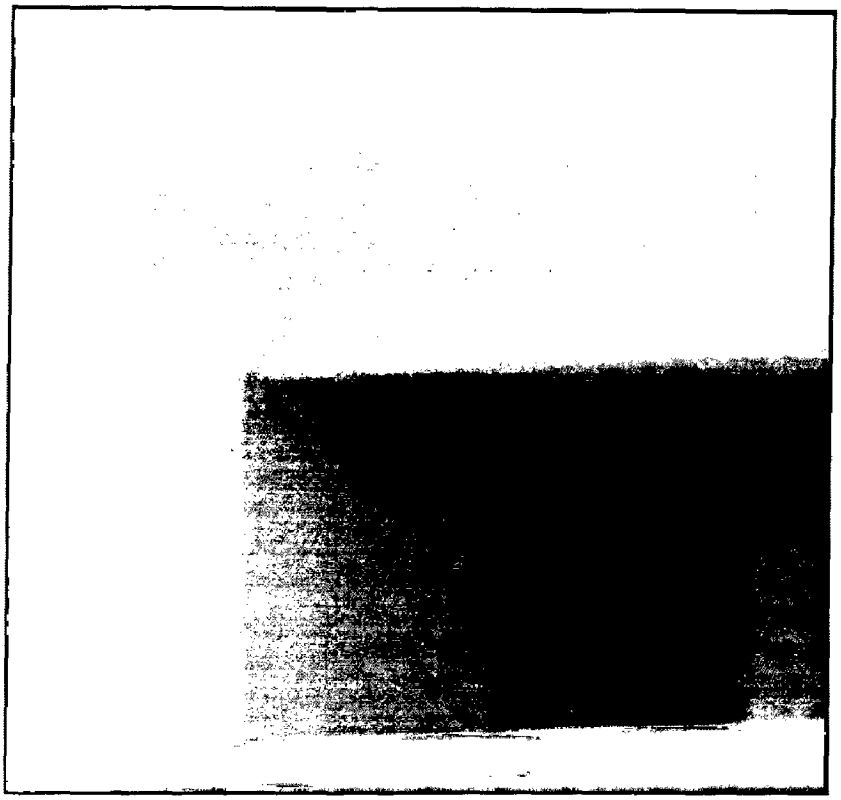

(g) Bicubic interpolation

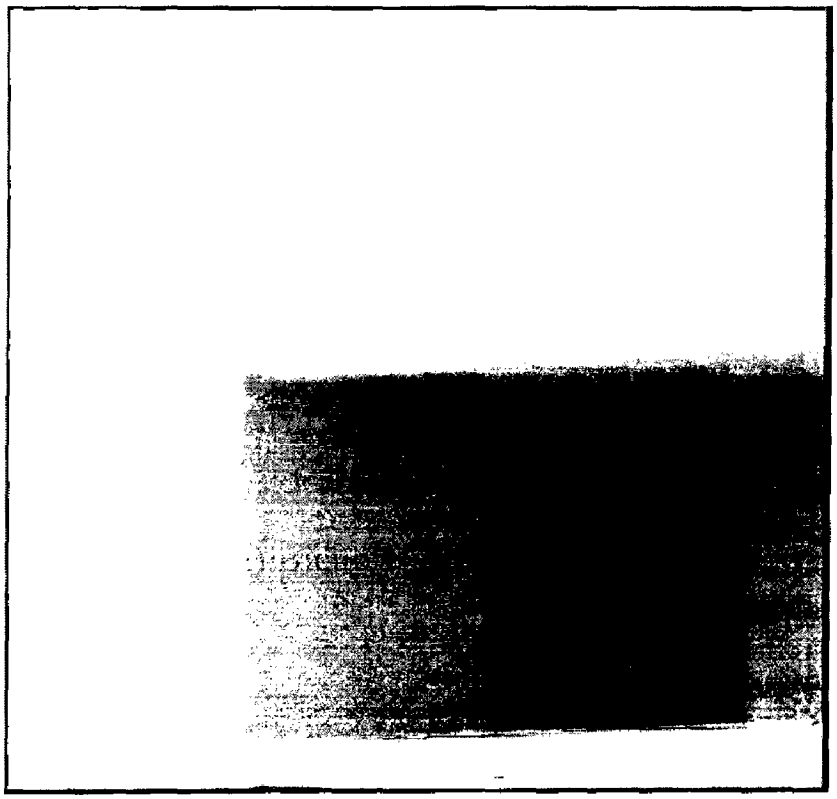

(h) Modified Frequency domain Multi-frame algorithm

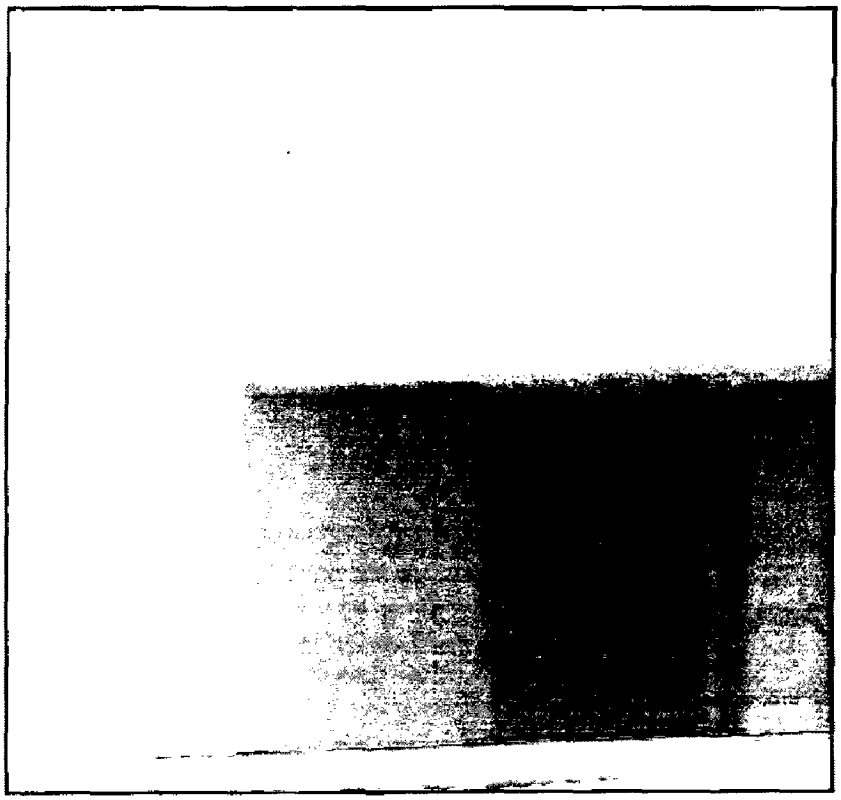

(i) Original HR image

Figure 5.2 (a), (b), (c), (d) set of low resolution images

(e) ---- Output of nearest neighbor interpolation

(f)----- Output of bilinear interpolation

(g)-----Output of bicubic interpolation

(h)--- Output of modified frequency domain approach

(i)---- Original high resolution image.

Motion Parameters

	Shift parameters		Rotation parameter
LR frames	Δx	Δy	θ
$im(1)$	**0**	**0**	**0**
$im(2)$	**-0.6349**	**0.0041**	**0**
$im(3)$	**-1.1412**	**-0.0347**	**0**
$im(4)$	**-1.7115**	**-0.0284**	**0**

Table 5.3

Error comparison

Type of technique	**Nearest neighbor**	**Bilinear interpolation**	**Bicubic interpolation**	**Implemented algorithm**
Error	**0.0878**	**0.0880**	**0.0878**	**0.04467**

Table 5.4

The shifts between the images are small and the rotation is negligible. The shifts are in terms of subpixel shifts of low resolution images. Since the shifts are evenly distributed over the 0-1 scale in x direction but not in y direction so we may bad quality of image variations in y directions using multiframe method. The error comparison table also suggests that. The error of the multiframe method is 50 percent less than the conventional bicubic interpolation method.

5.4 Data Set 3

A set of four low resolution images are taken for a constructed wall by taking the considerations explained above. Nikon Coolpix 5600'scamera is used for this dataset. The low resolution frames are taken by keeping picture size at 640*480. When ever we keep picture size like this some of the photo detectors in the camera will be inactive. For example in a horizontal direction photo detector array photo detector 1 will be active and photo detector 2, 3, 4 will be inactive again photo detector 5 will be active. So we will be able o achieve a low resolution image. At the same instant another image of the same scene wit double resolution is also taken at a picture size of 1280*960.

This image is having considerable variations through out it. Results of dataset are shown by the figure 5.3. In this figure (a), (b), (c), (d) are the set of misregistered and aliased images. Figure 5.3 (f) is the output of nearest neighborhood interpolation to double its resolution which uses only image $im(1)$ shown in figure 5.3(a) as input. Similarly figure 5.3(g), 5.3(h) are the outputs of bilinear and bicubic interpolations.

Finally figure 5.3(i) is the high resolution image from the multiframe modified frequency domain method and 5.3(j) is the original high resolution image directly taken from high resolution camera.

It has been found that the nearest neighbor hood interpolation producing an image having blocky appearance at some parts of the image. And linear interpolation is creating an output image affected by blur. Bicubic interpolation is producing a comparable picture with the high resolution image but still it is producing a considerable blur at high frequency edges.

Output of multiframe method is producing a good comparable image with the original high resolution image which is better than all the conventional interpolation techniques. The shift parameters between the low resolution images and the error functions of the constructed HR images with the original image are calculated and tabled in table 5.3 and 5.4.

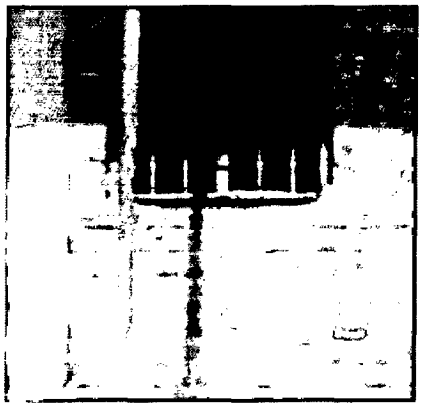

(a) LR frame 1 *im*(1)

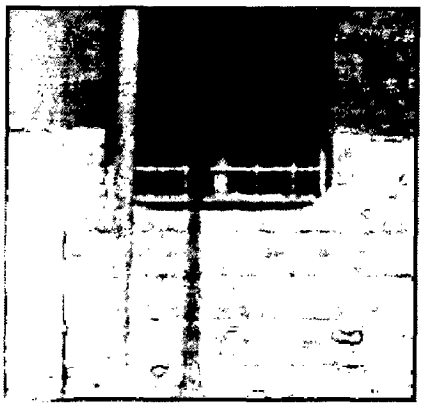

(b) LR frame 2 *im*(2)

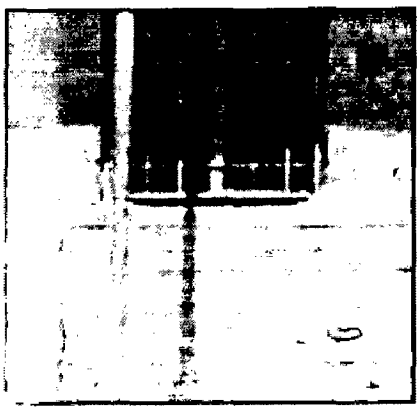

(c) LR frame 3 *im*(3)

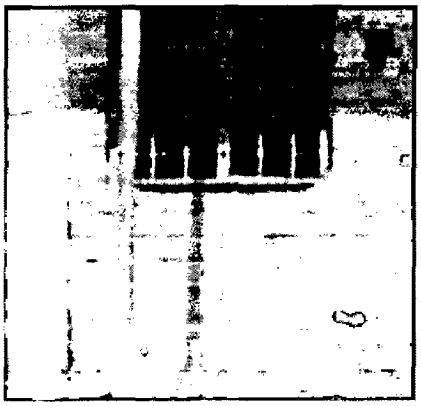

(d) LR frame 4 *im*(4)

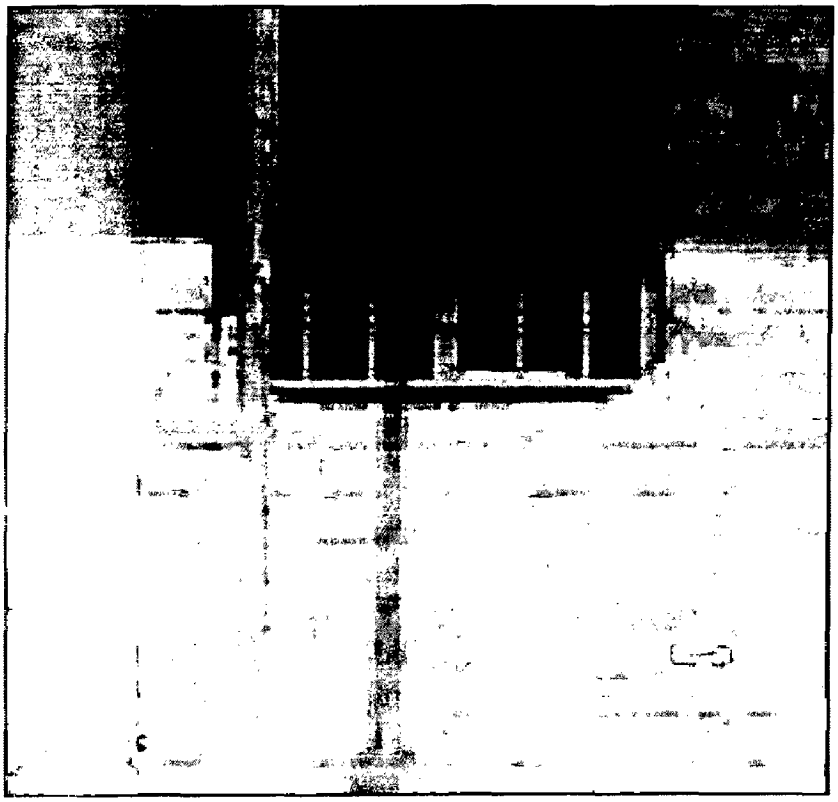

(e) O/P of nearest neighbor interpolation

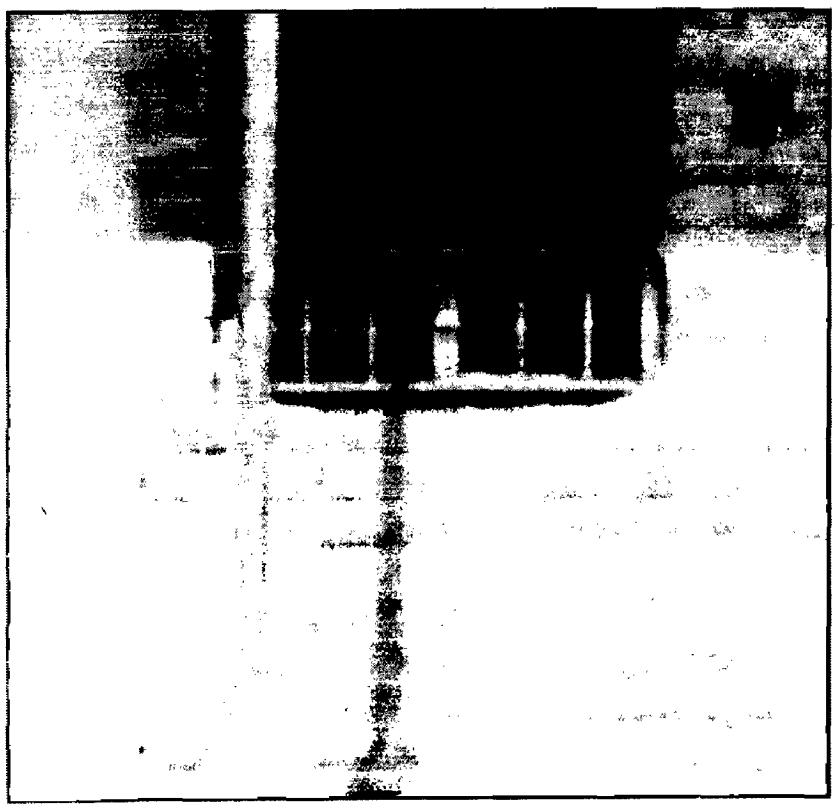

(f) O/P of Bilinear interpolation

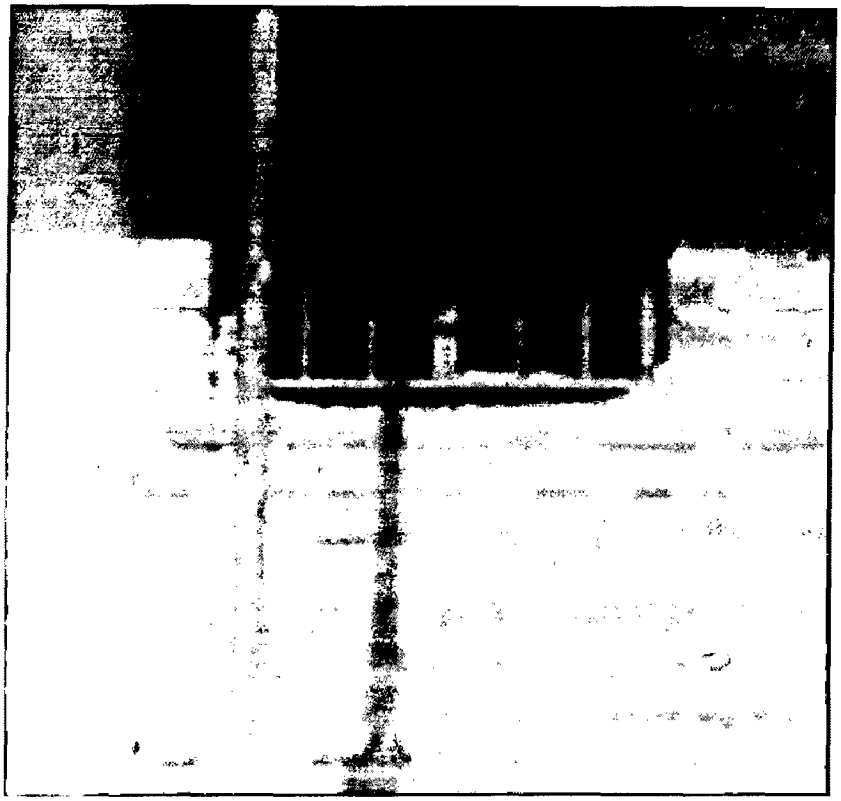

(g) O/P of Bicubic interpolation

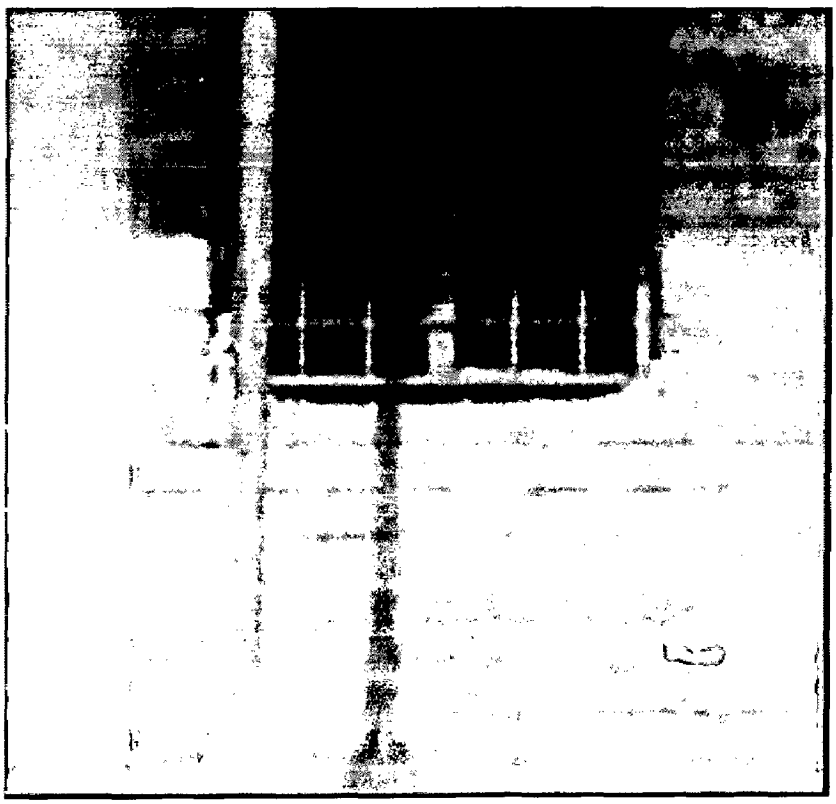

(h) O/P of Modified Frequency Domain Multi frame method

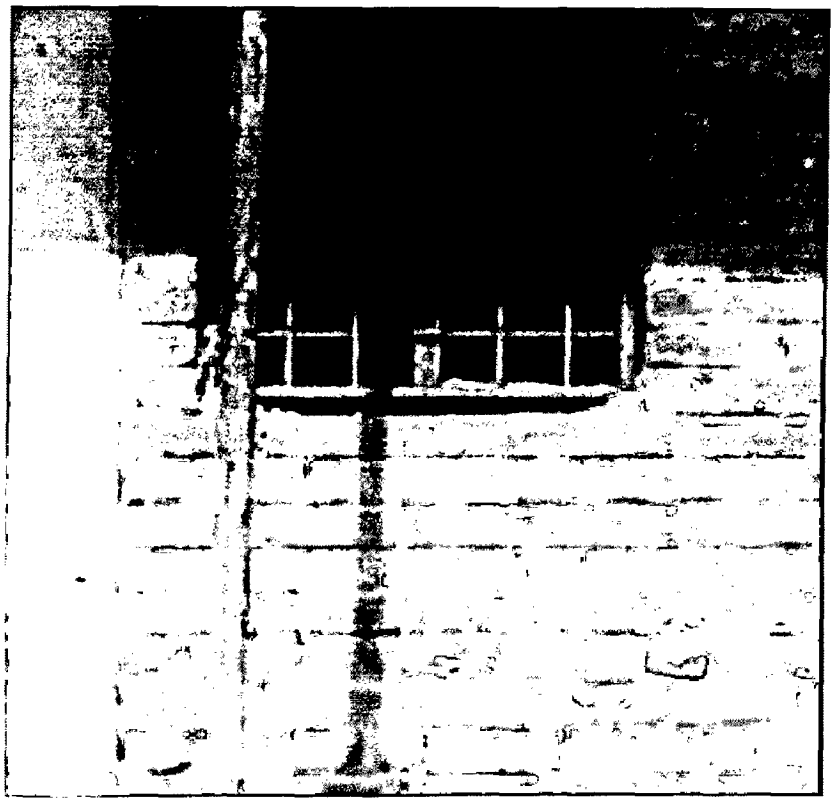

(i) Original HR image

Figure 5.3 (a), (b), (c), (d) set of low resolution images

(e) ---- Output of nearest neighbor interpolation

(f)----- Output of bilinear interpolation

(g)-----Output of bicubic interpolation

(h)--- Output of modified frequency domain approach

(i)---- Original high resolution image.

Motion Parameters

	Shift parameters		Rotation parameter
LR frames	Δx	Δy	θ
im(1)	**0**	**0**	**0**
im(2)	**-0.6626**	**1.4189**	**-0.1000**
im(3)	**0.2167**	**1.1951**	**-0.1000**
im(4)	**2.7045**	**-0.0358**	**0**

Table 5.5

Error comparison

Type of technique	**Nearest neighbor**	**Bilinear interpolation**	**Bicubic interpolation**	**Implemented algorithm**
Error	**0.1523**	**0.1419**	**0.1475**	**0.1255**

Table 5.6

The shifts between the images are small and the rotation is negligible. The shifts are in terms of subpixel shifts of low resolution images. Since the shifts are evenly distributed over the 0-1 scale in x direction but not in y direction so we may bad quality of image variations in y directions using multiframe method. The error comparison table also suggests that. The error of the multiframe method is 15 percent less than the conventional bicubic interpolation method.

5.4 Data set 4

The fourth dataset is taken from reference [16] is standard images to test super resolution algorithm. These images are having more frequency components.

In this figure (a), (b), (c), (d) are the set of misregistered and aliased images. Figure 5.4 (f) is the output of nearest neighborhood interpolation to double its resolution which uses only image *im*(1) shown in figure 5.4(a) as input. Similarly figure 5.4(g), 5.4(h) are the outputs of bilinear and bicubic interpolations. Finally figure 5.4(i) is the high resolution image from the multiframe modified frequency domain method.

The output of nearest neighbor interpolation is producing sharp edges, but still we can observe blocky appearance very clearly. Bilinear interpolation is producing blurred image as we can clearly seen. Bicubic interpolation is producing a somewhat better result than linear interpolation but some what less blurred. We can clearly see the out put of modified frequency domain algorithm is producing better result as compared to others. The mathematical it is not shown because there is no availability of original high-resolution image.

Output of multiframe method is producing a good comparable image with the original high resolution image which is better than all the conventional interpolation techniques. The shift parameters between the low resolution images are tabled in table 5.7.

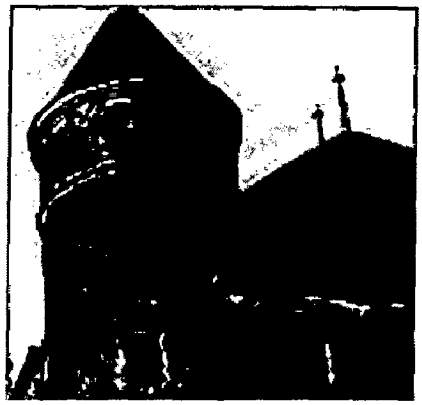

(a) LR frame 1 *im*(4)

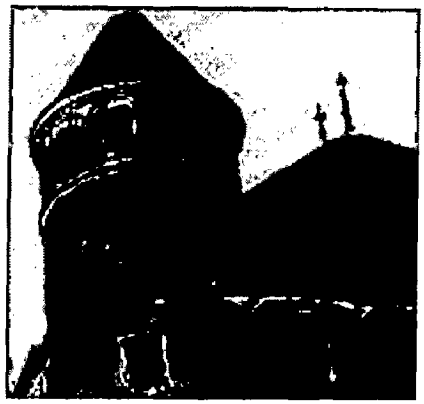

(b) LR frame 2 *im*(2)

(c) LR frame 3 *im*(3)

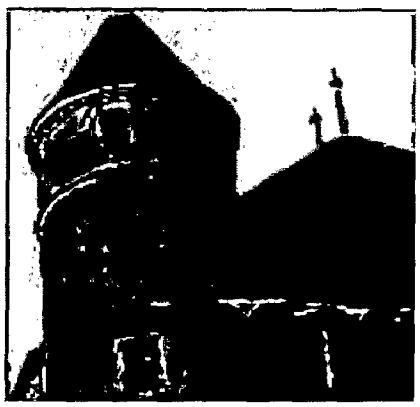

(d) LR frame 4 *im*(4)

(e) Nearest neighbor interpolation

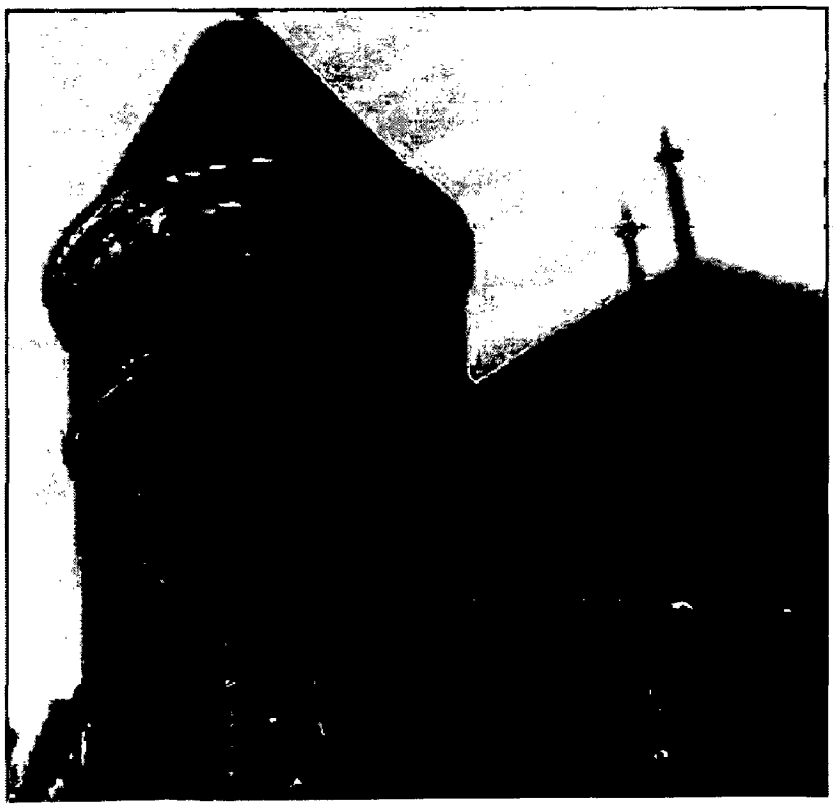

(f) Bilinear interpolation

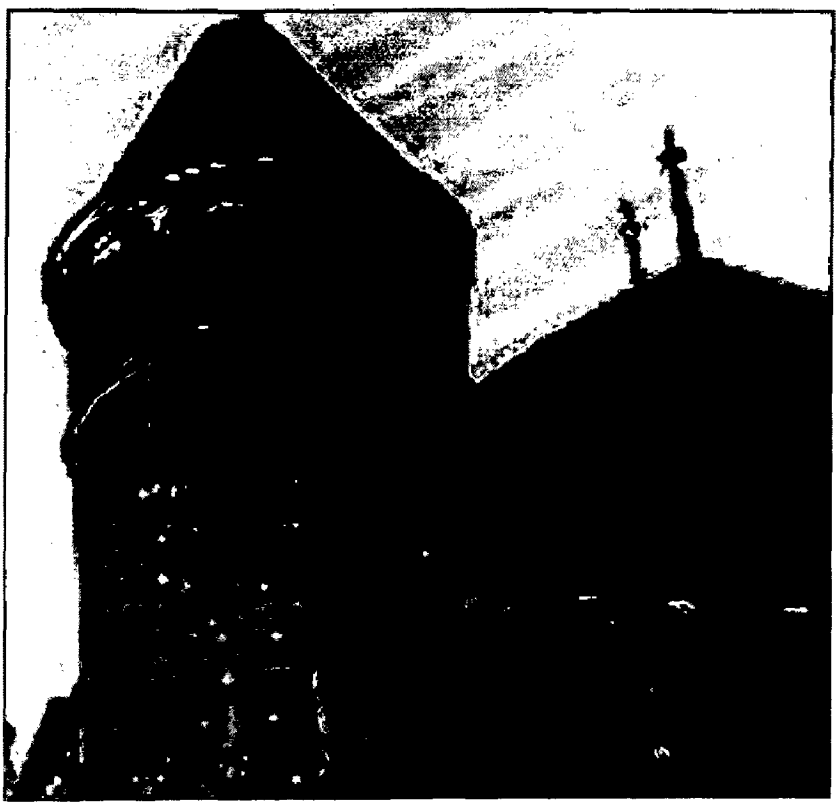

(g) Bicubic interpolation

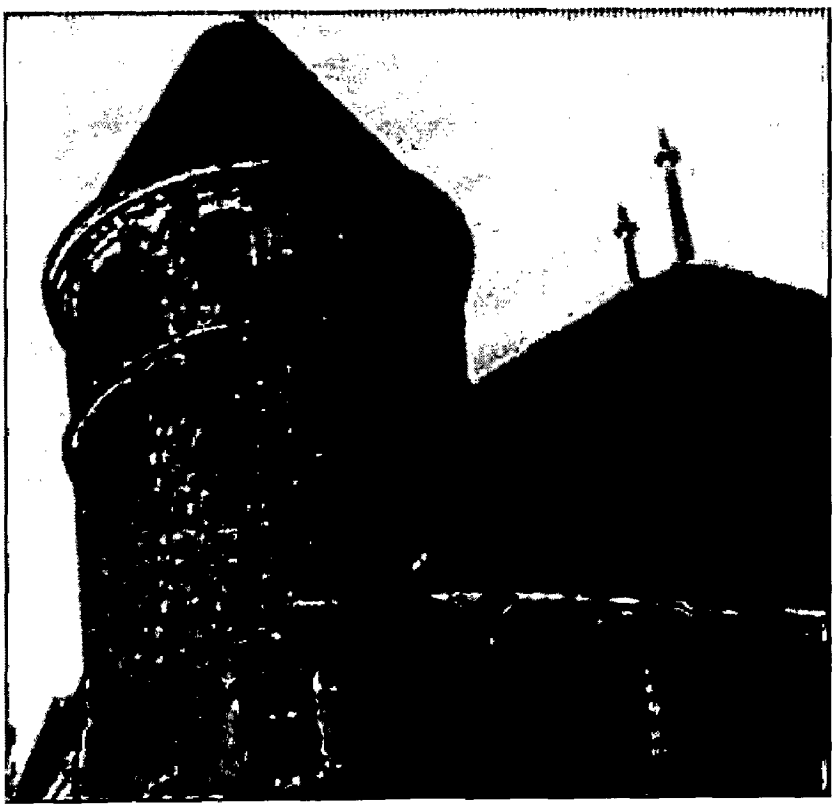

(h) Modified frequency domain multi frame method -Figure 5.4

Figure 5.4 (a), (b), (c), (d) set of low resolution images

(e) ---- Output of nearest neighbor interpolation

(f)----- Output of bilinear interpolation

(g)-----Output of bicubic interpolation

(h)--- Output of modified frequency domain approach

Motion Parameters

	Shift parameters		**Rotation parameter**
LR frames	Δx	Δy	θ
$im(1)$	**0**	**0**	**0**
$im(2)$	**-0.3027**	**-0.5451**	**0**
$im(3)$	**-0.4256**	**-0.6601**	**0**
$im(4)$	**-0.5680**	**-0.1140**	**0**

Table 5.7

5.5 Dataset 5

This dataset is a grey level dataset. Something like synthetic pattern. If we calculate the shift parameters manually it is of about 20-25 pixels in x direction and of around 10-15 pixels in y direction. And the image size is of order 200*200. So the subpixel shifts are very larger. This leads to misregistration means that the calculated rotation and shift parameters by the modified are wrong. Because of misregistration the output high resolution image by the modified frequency domain algorithm is distorted and shown in the figure 5.5(d).

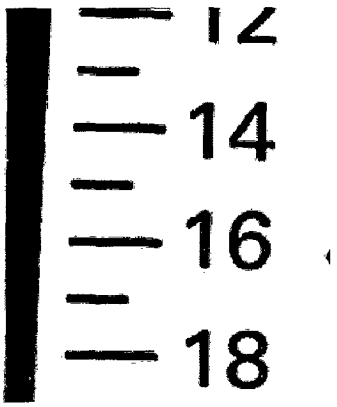

(a) LR frame 1 *im*(1)

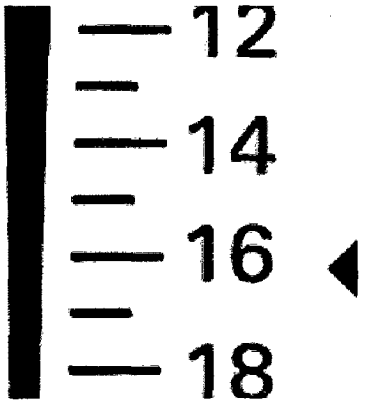

(b) LR frame 2 *im*(2)

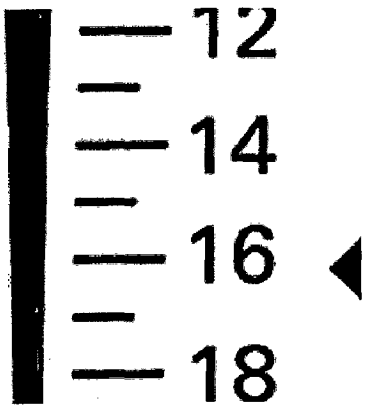

(c) LR frame 3 *im*(3)

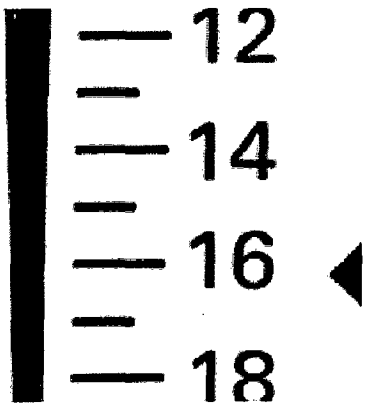

(d) LR frame 4 *im*(4)

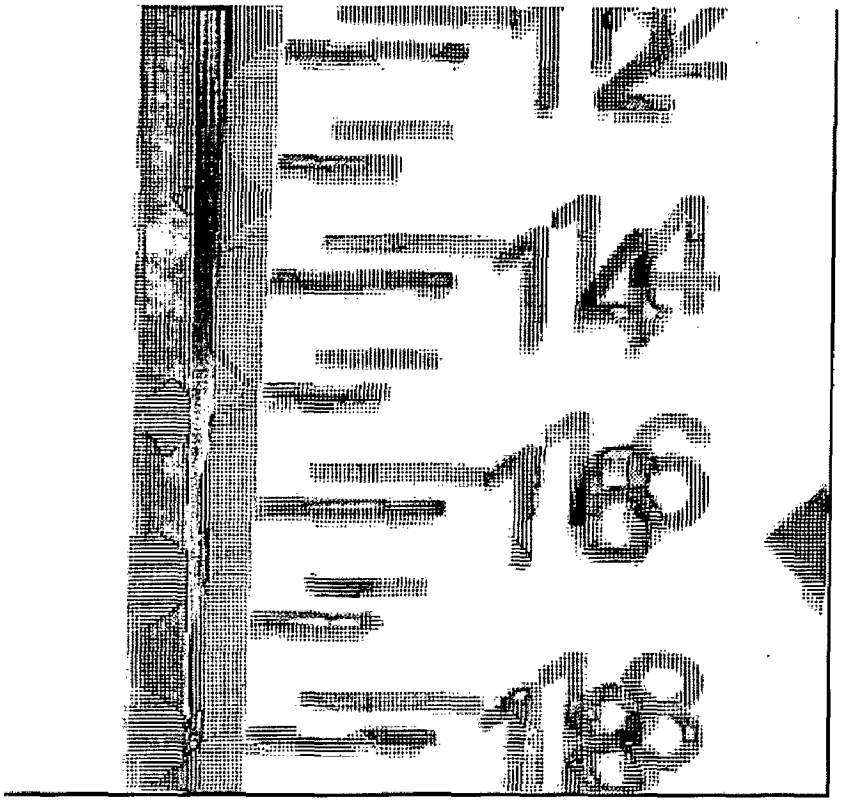

(e) HR frame from modified frequency domain multi frame algorithm

Figure 5.5 (a), (b), (c), (d) set of low resolution images ,

(e) ---- Output of modified frequency domain approach

The motion parameters between the low resolution images are tabled in the table 5.8.

Motion parameters

	Shift parameters		**Rotation parameter**
LR frames	Δx	Δy	θ
im(1)	**0**	**0**	**0**
im(2)	**-0.1469**	**0.2160**	**0.1000**
im(3)	**0.2266**	**0.1125**	**1.4000**
im(4)	**0.1627**	**0.0968**	**1.4000**

Table 5.8

Results of typical datasets are shown and discussed in the previous pages. It came to know that modified frequency domain algorithm is producing good results compared to the other conventional interpolation methods. Also I have observed that if the images having subpixel shifts which are spread over the range of 0-1 then we can expect a good result. For a set of 4 input images a best result would be obtained if the sub pixel shifts in both directions is differ by 0.25. That means first template image is shifted by $\delta_x = i + 0.25$, $\delta_y = i + 0.25$ with respect to and reference image, second template shifted by $\delta_x = i + 0.50, \delta_y = i + 0.50$ and third template image is shifted by $\delta_x = i + 0.75$, $\delta_y = i + 0.75$ with respect to the reference image, where i is a small integer.

But the results for data set 5 are not good. It is even giving worse output than the normal interpolation methods. This is because the shifts between the reference image and the template very large. When ever the shifts are large the results are not satisfactory because of misregistration. When ever the template images are having large shifts the registration algorithm will fail and the motions parameters that result from the algorithm will be wrong. Consequently the next block that is interpolation on to high resolution grid will also result a distorted image.

This modified frequency domain algorithm uses a one dimensional correlation for rotation estimation where as other multiframe methods will use two dimensional correlations. And the number of 2-D correlations used by the other methods is very large compared to the modified frequency domain method. The method used in this thesis work for shift estimations will not use correlations, where as the other registration methods use a large number of correlation methods. From the above tow reasons the computational complexity of this method is obviously decreased. Typically for an input image of size 100*100 the execution time of total algorithm is 2 minutes.

CHAPTER 6
CONCLUSION

This thesis work proposes a modified frequency domain method for the registration of a set of low-resolution, aliased images. Shift parameters in x and y directions and rotation angle θ are estimated by using the low frequency aliasing part of image. And the algorithm is checked over a set of fifteen datasets, after that we came to a conclusion that this algorithm is suited for datasets for which the planar shifts are small. This image registration technique is then applied to super-resolution imaging to reconstruct a double resolution image (in each dimension) from a set of aliased images.

After registering the low resolution images on to high resolution then the intensity values at pixels at high resolution grid are calculated using bicubic interpolation.

This output of modified frequency domain method is compared with the outputs of conventional interpolation methods and original high resolution image taken with a high resolution camera. Pixel to pixel difference between the constructed high resolution image and the original high resolution image are taken to find the error function.

This modified frequency domain algorithm uses a one dimensional correlation for rotation estimation where as other multiframe methods will use two dimensional correlations. And the number of 2-D correlations used by the other methods is very large compared to the modified frequency domain method. The method used in this thesis work for shift estimations will not use correlations, where as the other registration methods use a large number of correlation methods. From the above tow reasons the computational complexity of this method is obviously decreased.

Future work

The registration algorithm fails when the subpixel shifts between the reference image and template images are larger. This problem has to be fixed.

This registration algorithm does not allow the zooming between the reference image and the template image. This parameter also should be estimated in registration algorithm.

This algorithm does not compensate for the image blurring which is caused when the input images are taken when the camera is in motion. This blurring can be removed by a good deblurring algorithm.

Even though there is substantial decrease in the time complexity compared to other algorithms, this algorithm is still not suitable for real tie applications. The time complexity has to be still decreased.

REFERENCES

[1] Rafael C. Gonzalez, Richard E. Woods, Steven L. Eddins, "DIGITAL IMAGE PROCESSING USING MATLAB," Pearson education, 2004. sare

[2] Subhasis Chaudari (Editor), "SUPER-RESOLUTION IMAGING," The International Series in Engineering and Computer Science, volume 632, 2002.

[3] S.P.Kim ,N.K.Bose and H.M.Valenzuela , "Recursive Reconstruction of High Resolution Image From Noisy Undersampled Multiframes," IEEE transactions on Acoustics and Speech and Signal Processing, vol 38,pp.1013-1026,june.1990.

[4] Lisa Gottesfeld Brown, "A Survey of Image Registration Techniques," ACM Computing Surveys, Vol. 24, No. 4, December 1992.

[5] Patrick Vandewalle, Sabine S¨usstrunk and Martin Vetterli. "Superresolution images reconstructed from aliased images," LCAV - School of Computer and Communication Sciences Ecole Polytechnique F´ed´erale de Lausanne (EPFL) CH-1015 Switzerland.

[6] Patrick Vandewalle, Sabine S ¨ usstrunk and Martin Vetterli, "A Frequency Domain Approach to Registration of Aliased Images with Application to Super-resolution," Hindawi Publishing Corporation, EURASIP Journal on Applied Signal Processing, Volume 2006, Pages 1–14,2006.

[7] http://www.ph.tn.tudelft.nl/Courses/FIP/noframes/fip-Properti-2.html

[8] R. Y. Tsai and T. S. Huang, "Multiframe image restoration and registration," in Advances in computer Vision and Image Processing, vol. 1, chapter 7, pp. 317–339, JAI Press, Greenwich, Conn, USA, 1984.

[9] Michael Elad and Arie Feuer," Restoration of a Single Super Resolution Image from Several blurred noisy and undersampled measured images," IEEE transactions on image processing, vol.6, no.12, December 1997.

[10] S.P.Kim, N.K.Bose and H.M.Valenzuela,"Recursive reconstruction of high resolution image from noisy Undersampled multiframes" IEEE rtansactions on acoustics and speech signal processin, vol.38, no.6, june 1990.

[11] S. Borman and R. L. Stevenson, "Spatial resolution enhancement of low-resolution image sequences—a comprehensive review with directions for future research," Tech. Rep., Laboratory for Image and Signal Analysis (LISA), University of Notre Dame, Notre Dame, Ind, USA, 1998. Online available: http://www.nd.edu/□sborman/publications/.

[12] S.C. Park, M. K. Park, andM. G. Kang, "Super-resolution image reconstruction: a technical overview," IEEE Signal Processing Magazine, vol. 20, no. 3, pp. 21–36, 2003.

[13] B. S. Reddy and B. N. Chatterji, "An FFT-based technique for translation, rotation, and scale-invariant image registration," IEEE Transactions on Image Processing, vol. 5, no. 8, pp. 1266– 1271, 1996.

[14] H. Foroosh, J. B. Zerubia, and M. Berthod, "Extension of phase correlation to subpixel registration," IEEE Transactions on Image Processing, vol. 11, no. 3, pp. 188–200, 2002.

[15] L. Lucchese and G. M. Cortelazzo, "A noise-robust frequency domain technique for estimating planar roto-translations," IEEE Transactions on Signal Processing, vol. 48, no. 6, pp. 1769– 1786, 2000.

[16] http://www.hindawi.com/journals/asp/

[17] S.Peleg, D.Keren, and L.Schweitzer, "Improving image resolution using subpixel motion," Pattern recognition. Lett., Vol.5 , pp. 223-226, Mar,1987.

[18] Sina Farsiu, Dirk Robinson, Michael Elad, Peyman Milanfar, "Advances and Challenges in Super-Resolution," Wiley Periodicals, Inc., Vol. 14, pp-47–57, 2004.

[19] N.R. Shah and A. Zakhor, "Resolution enhancement of color video sequences," IEEE Trans. Image Processing, vol. 8, pp. 879-885, June 1999.

[20] N.K. Bose, H.C. Kim, and H.M. Valenzuela, "Recursive implementation of total least squares algorithm for image reconstruction from noisy, Undersampled Multiframes," in Proc. IEEE Conf. Acoustics, Speech and Signal Processing, Minneapolis, MN, Apr. 1993, vol. 5, pp. 269-272.

[21] S.P. Kim and W.Y. Su, "Recursive high-resolution reconstruction of blurred multiframe images," IEEE Trans. Image Processing, vol. 2, pp. 534-539, Oct. 1993.